Zeitschrift: Helvetica Physica Acta
Band: 40 (1967)
Heft: 6

Artikel: Finite nuclear size effects in internal conversion
Autor: Pauli, Hans-Christian
DOI: https://doi.org/10.5169/seals-113792

Finite Nuclear Size Effects in Internal Conversion

by **Hans-Christian Pauli**
Seminar für theoretische Physik der Universität Basel

(28. IV. 67)

Abstract. The process of internal conversion including finite nuclear size effects is reanalysed for an arbitrary multipole order. It can be shown that the dependence on nuclear structure can be described by two so called nuclear parameters which are—for a specific nuclear transition—independent of the atomic subshells. These parameters may be determined by two or three conversion experiments and checked by others. New formulas for the particle parameter and for the conversion coefficients and their dependence on these nuclear parameters are derived. A recalculation of the conversion coefficients and particle parameters including all finite nuclear size effects has been performed as well as a comparison with the conversion coefficients as computed by ROSE or by SLIV. The agreement with SLIV's values is generally better than with those of ROSE.

I. Introduction and Summary

An excited nucleus can decay by electromagnetic interactions. Internal conversion belongs to these processes and competes with the usual gamma transition inasmuch as the de-excitation takes place by the emission of an orbital electron instead of by the emission of a photon, especially at low energies. Assuming the gamma transition as the standard, the internal conversion transition probability W_e can be measured in units of the photon transition probability W_γ and this measure is the so called "internal conversion coefficient (ICC)" i.e.

$$\alpha = \frac{W_e}{W_\gamma} .$$

The internal conversion coefficient is a rather important tool for the determination of the multipolarity L as well as for the parity π of a nuclear transition. From these quantum numbers limitations on the spin and parities of the involved nuclear levels can be obtained.

In the first calculations of the internal conversion coefficients, as performed by ROSE [1] for the K-shell, neither the screening of the atomic electrons was taken into account nor the finite nuclear size, but the nucleus was assumed to be a point charge.

The renounciation of the latter assumption i.e. the introduction of the finite nuclear size leads to considerable corrections of the conversion coefficients. Firstly, the radial wave functions of the electrons have a completely different behaviour near the origin for a finite nucleus than for a point nucleus. Since the neighbourhood of the nucleus contributes a large part to the radial matrix elements this—so called static—effect is nonnegligible. Secondly, the correct treatment of the conversion matrix elements gives rise to additional matrix elements which disappear in a point nucleus approximation and wherein the operators of nuclear transition charges and

currents are explicitely contained. Thus, detailed nuclear structure enters in these additional terms and we shall call them dynamic in the following, contrary to the above mentioned static effects which depend only on static nuclear charge distribution. Especially for heavier nuclei the dynamic matrix elements may become important, and the measurement of conversion coefficients may contribute to the investigation of the dynamic nuclear structure.

The existence of nuclear structure effects in internal conversion—the so-called penetration—was first suggested by CHURCH and WENESER [2] for magnetic dipole ($M1$) transitions. In subsequent work the theory was extended to other multipolarities [3]. Calculations of the dynamic matrix elements were given only for the K-shell [4], and thus the considerations of CHURCH and WENESER had to be restricted on this shell. Nevertheless, penetration effects have to be expected also for the higher atomic shells. Particular work for L-subshell conversion coefficients has been done by CHURCH and WENESER [5] and KRAMERS and NILSSON [6], in order to explain the partially very large anomalies of the conversion coefficients which have been observed in hindered electric dipole ($E1$) transitions of low energy [7].

Although the theory of internal conversion including finite size effects is already scetched by the above mentioned authors, we shall present in this paper a complete and general reanalysis of the conversion process and obviously, repetitions can not always be avoided. The main aim we persue in this reanalysis is to separate properly the matrix elements which depend only on the electronic wave functions from those carrying the nuclear information. We will show, that all nuclear structure effects can be put into one nuclear parameter for magnetic and into two parameters for electric multipole transitions. These well defined parameters are independent of the subshells involved and can be determined by the measurement of one or two conversion coefficients or particle parameters and checked by others. Once these parameters are determined they should be verified by model dependent considerations.

Parallely to the investigation of the conversion coefficients we have reanalyzed the angular correlation for conversion electrons including finite size effects. For the standard γ-γ correlation we refer to the textbook literature [8] and restrict ourselves on the so-called particle parameter which includes all modifications of the standard theory through the introduction of conversion electrons. We shall present a considerable simpler notation for the general particle parameter than the formulas of BIEDENHARN and ROSE [9, 10, 11] or of IVASH [12], as well as explicit formulas for the particle parameters for the K, L_I, L_{II}, L_{III}, M_I, M_{II}, M_{III}, M_{IV}, N_I, ... subshells.

The investigation of nuclear structure by means of internal conversion presumes the knowledge of the static conversion coefficients. Today, two tabulations of internal conversion coefficients including the finite nuclear size are available.

The tabulation of ROSE [13] takes only the static effects of the finite nuclear size into account. SLIV and BAND [14] include also dynamic effects by means of the very rough model of the nuclear surface transition currents and charges. However, the discrepancies of these two tables are in many cases too large to be only due to these different assumptions. Such discrepancies can be expected to be significant only for magnetic low energy transitions. Therefore, they have to be attributed to numerical errors. In order to check their calculations we have performed a recalculation of the conversion coefficients for the K- and the L-shell with the same physical assumptions

as ROSE or SLIV. Although we agree very often with the values of ROSE within the combined limits of error, the agreement with SLIV's values is generally better, especially at low energies.

In the following, we discuss in Chapter II the formulation of the interaction and the separation of the general matrix elements into the static and dynamic parts. In Chapter III the formulas of the particle parameters are derived. The dynamic matrix elements are discussed in detail in Chapter IV, in order to simplify the theory by means of the definition of the nuclear parameter. Finally we give in Chapter V an outline of our numerical procedure as well as some selected numerical results.

II. Formulation of the Interaction

The total system consisting of the electron, the nucleus and the quantized radiation field is described in a zero order approximation by the Hamiltonian[1])

$$H_0 = H_n + H_\gamma + \boldsymbol{\alpha}\boldsymbol{p} + \beta + V(r_e) \tag{1}$$

where the two first terms represent the Hamiltonians of the free nucleus and the free radiation field. The latter terms in Eq. (1) represent the electron, moving in the central and static Coulomb potential. The interaction between the nucleus and electron occurs via the electro-magnetic field, which is usually divided into a transverse part, described by the vector potential $\boldsymbol{A}(\boldsymbol{r})$ for which $\operatorname{div}\boldsymbol{A} = 0$ (solenoidal fields), and a longitudinal part causing the instanteous Coulomb interaction. With this gauge any divergencies can be avoided [15]. Since the point charge interaction is already contained in the unperturbed Hamiltonian, the interaction Hamiltonian is given by

$$H_{int} = \int d\tau \left(\boldsymbol{j}_n(\boldsymbol{r}) + \boldsymbol{j}_e(\boldsymbol{r})\right) \boldsymbol{A}(\boldsymbol{r}) + \int d\tau\, d\tau' \frac{\varrho_n(\boldsymbol{r})\, \varrho_e(\boldsymbol{r}')}{|\boldsymbol{r}-\boldsymbol{r}'|} - V(r) \tag{2}$$

where $\boldsymbol{j}(\boldsymbol{r})$ and $\varrho(\boldsymbol{r})$ are the transition currents and charges of the nucleus and the electron.

The vector potential $\boldsymbol{A}(\boldsymbol{r})$ is expanded into multipole components according to [15]

$$\boldsymbol{A}(\boldsymbol{r}) = \sum_q \sum_{\substack{LM \\ L\geqslant 1}} \sqrt{\frac{4\pi q}{R}} \cdot \{a_{LM}(E)\, \boldsymbol{A}_{LM}(E) + a_{LM}(M)\, \boldsymbol{A}_{LM}(M) + c.\,c.\} \tag{3}$$

where the electric (E) and magnetic (M) multipole fields are given by [16]

$$\begin{aligned} \boldsymbol{A}_{LM}(M) &= \frac{\boldsymbol{L}}{\sqrt{L\,(L+1)}}\, j_L(q\,r)\, i^L\, Y_{LM}(\hat{r}) \\ \boldsymbol{A}_{LM}(E) &= -\frac{1}{q} \cdot \frac{\boldsymbol{\nabla} \times \boldsymbol{L}}{\sqrt{L\,(L+1)}}\, j_L(q\,r)\, i^L\, Y_{LM}(\hat{r})\,. \end{aligned} \tag{4}$$

For the spherical Bessel functions $j_L(q \cdot r)$ we use the same notation as SCHIFF [17].

The multipole fields, enclosed in a large sphere of radius R, can be understood as photons with angular momentum L and magnetic quantum number M, wave number q, parity $(-)^L$ and $(-)^{L+1}$ for electric and magnetic fields, respectively, and obey the "convention T" i.e. they are transformed under time-reversal-operation T as

$$T\,|\,j\,\mu\rangle = (-)^{j-\mu}\,|\,j\,-\,\mu\rangle\,.$$

[1]) Here and afterwards relativistic units are used throughout ($\hbar = c = 1$, $m_e = 1$, i.e. $e^2 = \alpha \cong 1/137$.

With the normalization (3) the destruction and creation operators, a_{LM} and a^+_{LM}, have the only nonvanishing matrix elements

$$\langle n \mid a_{LM} \mid n+1\rangle = \langle n+1 \mid a^+_{LM} \mid n\rangle = \sqrt{n+1}$$

where $\mid n\rangle$ represents an eigenstate with n photons in question.

In order to evaluate the transition amplitudes we consider a transition from an initial state $\mid i\rangle$ where the nucleus is in the excited and the electron in the ground (or bound) state, to a final state $\mid f\rangle$, where the nucleus has transferred the energy k to the electron. The eigenfunctions of Eq. (1) for the nucleus are represented by φ and for the electron by ψ. The transition matrixelement of the Coulomb interaction (third term in (2)) is calculated by first order perturbation theory and that of the current interaction by second order according to an emission and reabsorption of a photon. Thus we have

$$H_{int} = \langle \varphi_f \psi_f \mid \frac{\varrho_n(\boldsymbol{r})\,\varrho_e(\boldsymbol{r}')}{\mid \boldsymbol{r}-\boldsymbol{r}' \mid} - V(r_e) \mid \varphi_i \psi_i\rangle + \sum \sqrt{\frac{4\pi q}{R}} \cdot \left\{ \frac{\langle \varphi_f \mid \boldsymbol{j}_n \boldsymbol{A}_{LM}(\pi) \mid \varphi_i\rangle \langle \psi_f \mid \boldsymbol{j}_e \boldsymbol{A}^+_{LM}(\pi) \mid \psi_i\rangle}{q-k} + \frac{\langle \varphi_f \mid \boldsymbol{j}_n A_{LM}(\pi) \mid \varphi_i\rangle \langle \psi_f \mid \boldsymbol{j}_e \boldsymbol{A}^+_{LM}(\pi) \mid \psi_i\rangle}{q+k} \right\} . \tag{5}$$

The summation over q can be evaluated, replacing $\sum_q$ by $\int dq\ R/\pi$ and using the relations [18]

$$\int_0^\infty dq\, \frac{q^2}{q^2-k^2}\, j_L(q\,r)\, j_L(q\,r') = i\,\frac{\pi k}{2}\, j_L(k\,r_<)\, h_L(k\,r_>) \tag{6a}$$

and

$$\int_0^\infty dq\, \frac{1}{q^2-k^2}\, j_L(q\,r)\, j_L(q\,r') = i\,\frac{\pi}{2k}\, j_L(k\,r_<)\, h_L(k\,r_>) - \frac{\pi}{2k} \cdot \frac{r_<^L\, r_>^{-L-1}}{(2L+1)} . \tag{6b}$$

In the above formula $h_L(kr)$ is the spherical Hankel function [17] and $r_<$, $r_>$ are the smaller or greater of r and r', respectively. Since magnetic and electric multipole fields have different parity and different selection rules, it will be useful to split up the total amplitude into the magnetic and electric components and to discuss each part separately, i.e.

$$H_{int} = \sum_{\substack{L,M \\ L\geqslant 1}} H_{LM}(M) + \sum_{\substack{L,M \\ L\geqslant 1}} H_{LM}(E) + H\,(E,\, L=0) . \tag{7}$$

The last term represents the so called monopole transition amplitude.

Since the transition amplitude is easier to handle in the magnetic than in the electric case, we start with the magnetic amplitudes.

Magnetic Multipole Transitions

Inserting (4) and (6a) in Eq. (5)[2] we obtain

$$H_{LM}(M) = \frac{4\pi i k}{L\,(L+1)} \int_0^\infty d\tau_n\, d\tau_e\, [\boldsymbol{j}\, \boldsymbol{L}\, i_L\, Y_{LM}]^+_n\, [\boldsymbol{j}\, \boldsymbol{L}\, i^L\, Y_{LM}]_e\, j_L(k\,r_<)\, h_L(k\,r_>) . \tag{8}$$

[2] The symbol $\int_0^r d\tau$ means an integration over a sphere of radius r.

It is suitable to construct the matrixelements in the way that always $r_n \geqslant r_e$, since we have much more knowledge of electronic than about nucleonic variables. Therefore we write for (8)

$$H_{LM}(M) = \frac{4\pi i k}{L(L+1)} \left\{ \int_0^\infty d\tau_n [\boldsymbol{j}_n \boldsymbol{L} i^L Y_{LM}]^+ j_L(kr) \int_0^\infty d\tau_e [\boldsymbol{j}_e L i^L Y_{LM}] h_L(kr) \right.$$
$$+ \int_0^\infty d\tau_n [\boldsymbol{j}_n \boldsymbol{L} i^L Y_{LM}]^+ h_L(kr) \int_0^{r_n} d\tau_e [\boldsymbol{j}_e \boldsymbol{L} i^L Y_{LM}]_e j_L(kr)$$
$$\left. - \int_0^\infty d\tau_n [\boldsymbol{j}_n \boldsymbol{L} i^L Y_{LM}]^+ j_L(kr) \int_0^{r_n} d\tau_e [\boldsymbol{j}_e \boldsymbol{L} i^L Y_{LM}] h_L(kr) \right\}. \quad (9)$$

In the first term of this equation the nucleonic and electronic variables are separated exactly and the pure nucleonic integral is just the matrix element of a radiative ML transition. The second and third terms are the so called penetration terms, where such a factorability is not possible. Obviously the penetration terms disappear in the approximation of a point nucleus. We denote the first term in Eq. (9) as static and the penetration terms as dynamic matrix element since the latter depends explicitely on a dynamic nuclear model. It is useful to have the gamma transition amplitude as an overall factor and thus we write

$$H_{LM}(M) = 4\pi i k \int_0^\infty d\tau_n \boldsymbol{j}_n \boldsymbol{A}^+_{LM}(M) M_{LM}(M) \quad (10)$$

where the magnetic multipole field $\boldsymbol{A}_{LM}(M)$ is defined in Eq. (4). In Eq. (10) we have chosen the notation

$$M_{LM}(M) = M^{(s)}_{LM} + M^{(d)}_{LM}(M) \quad (11)$$

with

$$M^{(s)}_{LM}(M) = \int_0^\infty d\tau_e \frac{\boldsymbol{j}_e \boldsymbol{L}}{\sqrt{L(L+1)}} i^L Y_{LM} h_L(kr). \quad (12)$$

$$M^{(d)}_{LM}(M) = \frac{\int_0^\infty d\tau_n [\boldsymbol{j}_n \boldsymbol{L} i^L Y_{LM}]^+ \left\{ h_L \cdot \int_0^{r_n} d\tau_e \boldsymbol{j}_e \boldsymbol{L} i^L Y_{LM} j_L - j_L \int_0^{r_n} d\tau_e \boldsymbol{j}_e \boldsymbol{L} i^L Y_{LM} h_L(kr) \right\}}{\sqrt{L(L+1)} \int_0^\infty d\tau_n [\boldsymbol{j}_n \boldsymbol{L} i^L Y_{LM}]^+ j_L(kr)} \quad (13)$$

where the indices (s) or (d) stand for "static" or "dynamic" matrix elements.

Electric Multipole Transitions

The amplitude of an electric transition is obtained in a similar manner as in the magnetic case, but the formulas are much more complicated. In precise analogy to Eq. (8) we get from Eq. (5) using Eqs. (4) and (6b)

$$H_{LM}(E) = \frac{4\pi i}{k L(L+1)} \int d\tau_n d\tau_e [\boldsymbol{j} (\boldsymbol{\nabla} \times \boldsymbol{L}) i^L Y_{LM}]^+_n [\boldsymbol{j} (\boldsymbol{\nabla} \times \boldsymbol{L}) i^L Y_{LM}]_e j_L(kr_<) h_L(kr_>)$$
$$- \frac{4\pi}{k^2 L(L+1)(2L+1)} \int d\tau_n d\tau_e [\boldsymbol{j} (\boldsymbol{\nabla} \times \boldsymbol{L}) i^L Y_{LM}]^+_n [\boldsymbol{j} (\boldsymbol{\nabla} \times \boldsymbol{L}) i^L Y_{LM}]_e$$
$$\times r_<^L r_>^{-L-1}. \quad (14)$$

This matrix element can be evaluated further by use of the well-known gradient formula

$$\boldsymbol{\nabla} \times \boldsymbol{L} = -i \left[\boldsymbol{r} \Delta - \boldsymbol{\nabla} \frac{\partial}{\partial r} r \right].$$

The operator $\boldsymbol{j}(r) \cdot \boldsymbol{\nabla}$ can be integrated by parts in order to use the continuity equation

$$\boldsymbol{\nabla} \boldsymbol{j}_e + i\, k\, \varrho_e = 0 \qquad \boldsymbol{\nabla} \boldsymbol{j}_n - i\, k\, \varrho_n = 0\,.$$

After some straight forward calculations we get

$$H_{LM}(E) = 4\,\pi\, i\, k \left\{ \iint_0^\infty d\tau_e\, d\tau_n\, Q_n^+\, Q_e\, j_L(k\, r_<)\, h_L(k\, r_>) \right.$$

$$\left. - \frac{i}{k} \int_0^\infty d\tau_n \boldsymbol{j}_n \boldsymbol{r}_n (i^L\, Y_{LM})^+ \oint\limits_{r_e = r_n} d\tau_e\, \boldsymbol{j}_e\, \boldsymbol{r}\, (i^L\, Y_{LM}) \right\}$$

$$- \frac{4\,\pi}{(2\,L+1)} \iint d\tau_n\, d\tau_e\, \varrho_n\, \varrho_e\, (i^L\, Y_{LM})^+\, (i^L\, Y_{LM})\, r_<^L\, r_>^{-L-1} \tag{15}$$

where we have introduced the operator

$$Q_e = \frac{1}{\sqrt{L\,(L+1)}} \left[i\, k\, \boldsymbol{j}_e\, \hat{r} - \varrho_e \frac{\partial}{\partial r} r \right] i^L\, Y_{LM} \tag{16a}$$

$$Q_n = \frac{1}{\sqrt{L\,(L+1)}} \left[i\, k\, \boldsymbol{j}_n\, \hat{r} - \varrho_n \frac{\partial}{\partial r} r \right] i^L\, Y_{LM}\,. \tag{16b}$$

In the derivation of this result we have made use of the identity

$$j_L(x)\, h_{L-1}(x) - j_{L-1}(x)\, h_L(x) = \frac{i}{x^2}$$

and their derivatives.

It can now be seen at once that the last term in (15) cancels the corresponding term of the multipole expansion of the Coulomb matrix elements in Eq. (2). Since the expansion of the radiative field has no component $L = 0$, this term remains and gives rise to the monopole term as discussed e.g. in ref. [3]. In the present paper we shall neglect this monopole term since the strange surface integral in (15) is caused by the integration by parts and not only non-negligible but in fact dominant, as will be discussed in chapter IV. The further procedure is in precise analogy to the magnetic case.

We write the pure transition amplitude
i.e.

$$\int_0^\infty d\tau_n\, Q_n^+\, j_L(k\, r) = \int_0^\infty d\tau_n \boldsymbol{j}_n\, \boldsymbol{A}_{LM}^+(E)$$

as an overall factor of the electric matrix element and get

$$H_{LM}(E) = 4\,\pi\, i\, k \int_0^\infty d\tau_n \boldsymbol{j}_n\, \boldsymbol{A}_{LM}^+(E)\, M_{LM}(E) \tag{17}$$

where we have used the following notation

$$M_{LM}(E) = M^{(s)}_{LM}(E) + M^{(d)}_{LM}(E) \tag{18}$$

with

$$M^{(s)}_{LM}(E) = \int_0^\infty d\tau_e \, Q_e \, h_L(k\,r) \tag{19a}$$

$$M^{(d)}_{LM}(E) = \frac{-\frac{i}{r}\int_0^\infty d\tau_n \, \boldsymbol{j}_n \boldsymbol{r} \, (i^L Y_{LM})^+ \oint_{r_e=r_n} d\Omega \, \boldsymbol{j}_e \boldsymbol{r} \, i^L Y_{LM} + \int_0^\infty d\tau_n \, Q_n^+ \left\{ h_L \int_0^{r_n} d\tau_e \, Q_e \, j_L - j_L \int_0^{r_n} d\tau_e \, Q_e \, h_L \right\}}{\int_0^\infty d\tau_n Q_n^+ \, j_L(k\,r)} . \tag{19b}$$

The index (s) stands for "static" and (d) for "dynamic" matrix elements.

III. Density Matrix Formalism

The aim of this chapter is to deduce the density matrix of the conversion process in order to get so called general or normalized particle parameters through comparison with the normal density matrix for a gamma transition.

In the former chapter we have calculated the general transition amplitude in terms of transition currents and charges. In order to specify the different states, let us introduce explicit quantum numbers. The nucleus is initially in the excited and randomly oriented state with spin I_i, and decays into the final state described by the quantum spin number I_f, M_f under emission of an electron. The electron is characterised in the initial state by the Dirac quantum number $\varkappa_i$, with random spin orientation μ_i, and in the final state by the wave number p and the intrinsic polarisation τ. Thus we have

$$H_{int} = 4\,\pi\,i\,k \sum_{\pi L M} \langle I_f M_f \,|\, \boldsymbol{j}_n \, A^+_{LM}(\pi) \,|\, I_i M_i \rangle \, \langle \boldsymbol{p}, \tau \,|\, M_{LM}(\pi) \,|\, \varkappa_i \mu_i \rangle . \tag{20}$$

The final state of the electron can be expanded into the standing wave solutions $|\, \varkappa\mu \rangle$, which are eigensolutions of the Dirac equation, i.e.

$$|\, \boldsymbol{p}, \tau \rangle = \sum_{\varkappa \mu} s_\varkappa \, a_{\varkappa\mu}(\tau) \,|\, \varkappa\,\mu \rangle$$

where s_x and $a_{x\mu}$ is defined in the appendix by Eq. (A 12). Thus, equation (20) becomes

$$H_{int} = 4\,\pi\,i\,k \sum_{\pi L M \varkappa \mu} \langle I_f M_f | \, \boldsymbol{j}_n \, \boldsymbol{A}^+_{LM}(\pi) \,|\, I_i M_i \rangle \, s^+_\varkappa \, a^+_{\varkappa\mu}(\tau) \, \langle \varkappa\,\mu \,|\, M_{LM}(\pi) \,|\, \varkappa_i \mu_i \rangle \tag{21}$$

and the density matrix can be written

$$\begin{aligned} \langle M'_f \,|\, \varrho \,|\, M_f \rangle = \sum_{\substack{M_i, \mu_i, \tau \\ \pi L M \varkappa \mu \\ \pi' L' M' \varkappa' \mu'}} & s^+_\varkappa \, s_{\varkappa'} \, a^+_{\varkappa\mu}(\tau) \, a_{\varkappa'\mu'}(\tau) \\ & \cdot \langle \varkappa'\,\mu' \,|\, M_{L'M'}(\pi') \,|\, \varkappa_i \mu_i \rangle^+ \, \langle \varkappa\,\mu \,|\, M_{LM}(\pi) \,|\, \varkappa_i \mu_i \rangle \\ & \cdot \langle I_f M_f | \, \boldsymbol{j}_n \, \boldsymbol{A}^+_{LM}(\pi) \,|\, I_i M_i \rangle \, \langle I_f M'_f | \, \boldsymbol{j}_n \, \boldsymbol{A}^+_{L'M'}(\pi') \,|\, I_i M_i \rangle^+ . \end{aligned} \tag{22}$$

The summation over the polarization τ can be carried out as well as the summation over the remaining azimuthal quantum numbers μ_i, μ, μ', of the electron. We use the Wigner-Eckart theorem [19], and introduce reduced matrix elements according to

$$\langle \varkappa\, \mu \mid M_{L\,M}(\pi) \mid \varkappa_i\, \mu_i \rangle = (-)^{j-\mu} \begin{pmatrix} j_i & L & j \\ \mu_i & M & -\mu \end{pmatrix} \langle \varkappa \parallel \pi\, L \parallel \varkappa_i \rangle \,. \tag{23}$$

Together with Eqs. (A 22) and (A 23) in the appendix, the relation

$$\begin{aligned} &\sum_{\tau,\mu,\mu',\mu_i} (-)^{j-\mu+j'-\mu'} \begin{pmatrix} j_i & L & j \\ \mu_i & M & -\mu \end{pmatrix} \begin{pmatrix} j_i & L' & j' \\ \mu_i & M' & -\mu' \end{pmatrix} a^{+}_{\varkappa\mu}(\tau) a_{\varkappa'\mu'}(\tau) \\ &= \frac{1}{4\pi} \sum_{kq} (-)^{M} (2k+1)\, D^{k}_{oq} \begin{pmatrix} L & L' & k \\ M & -M' & -q \end{pmatrix} (-)^{j_i+1/2} \sqrt{(2j+1)(2j'+1)} \\ &\times \begin{pmatrix} j & j' & k \\ 1/2 & -1/2 & 0 \end{pmatrix} \begin{Bmatrix} j & j' & k \\ L' & L & j_i \end{Bmatrix} \end{aligned}$$

can be derived.

The density matrix can now be written in the final form

$$\begin{aligned} \langle M'_f \mid \varrho \mid M \rangle = &\sum_{\substack{k q L L' \pi \pi' \\ M_i M M'}} (-)^{L+L'+M+1} (2k+1)\, D^{k}_{oq} \begin{pmatrix} L & L' & k \\ 1 & -1 & 0 \end{pmatrix} \begin{pmatrix} L & L' & k \\ M & -M' & -q \end{pmatrix} \\ &\times \langle I_f\, M_f \mid \boldsymbol{j}_n\, \boldsymbol{A}^{+}_{L\,M}(\pi) \mid I_i\, M_i \rangle \langle I_f\, M'_f \mid \boldsymbol{j}_n\, \boldsymbol{A}^{+}_{L'\,M'}(\pi') \mid I_i\, M_i \rangle^{+} \\ &\times \sqrt{(2L+1)(2L'+1)}\; B_k(\pi L, \pi' L') \,. \end{aligned} \tag{24}$$

This represents the density matrix of a pure gamma transition up to the factor B_k, which we shall call the non normalized particle parameter for internal conversion.

This particle parameter B_k $(\pi L, \pi' L')$ is defined by

$$\begin{aligned} B_k(\pi L, \pi' L') = (-)^{j_i - 1/2} &\sum_{\varkappa,\varkappa'} \sqrt{(2j+1)(2j'+1)}\; \frac{\begin{pmatrix} j & j' & k \\ 1/2 & -1/2 & 0 \end{pmatrix} \begin{Bmatrix} j & j' & k \\ L' & L & j_i \end{Bmatrix}}{\begin{pmatrix} L & L' & k \\ 1 & -1 & 0 \end{pmatrix}} \\ &\times Q_{\varkappa\varkappa_i}(\pi L)\; Q^{+}_{\varkappa\varkappa_i}(\pi' L') \end{aligned} \tag{25}$$

with

$$Q_{\varkappa\varkappa_i}(\pi L) = (-)^{L}\, 2\pi \sqrt{\frac{\alpha\, k}{(2L+1)}}\; s^{+}_{\varkappa} \langle \varkappa \parallel \pi L \parallel \varkappa_i \rangle \,. \tag{26}$$

For the special case $k = 0$, the particle parameter B_0 is just the conversion coefficient, i.e. for electric multipoles

$$\alpha_L = \sum_{\varkappa} \mid Q_{\varkappa\varkappa_i}(E\,L) \mid^2 = B_0(E\,L, E\,L) \tag{27}$$

while for magnetic multipoles

$$\beta_L = \sum_{\varkappa} \mid Q_{\varkappa\varkappa_i}(M\,L) \mid^2 = B_0(M\,L, M\,L) \,. \tag{28}$$

The particle parameter [9] is normalized corresponding to

$$b_0 = 1$$

and we define thus the normalized particle parameter to be

$$b_k(\pi L, \pi' L') = \frac{B_k(\pi L, \pi' L')}{\sqrt{B_0(\pi L, \pi L)\, B_0(\pi' L', \pi' L')}} \tag{29}$$

Further Investigation of the Particle Parameter

The geometry factor of particle parameter does not depend neither on the angular momentum l nor on the sign of $\varkappa$, and we can handle the magnetic and electric transitions simultaneously. Although every wanted particle parameter can be obtained by the general formula (29), we will go more into detail, in order to clarify the dependence on the tensor parameter k, at least in the simplier cases.

First, we shall consider *pure multipoles* only, i.e. $L = L'$. For the K, L_I, L_{II}, M_I, M_{II} shell, i.e. for $j_i = {}^1/_2$, the normalized particle parameter b_k can be written by use of Eq. (A 28) as

$$b_k(\pi L, \pi L) = 1 + \frac{k\,(k+1)}{2\,L\,(L+1) - k\,(k+1)} \frac{1}{2\,(2\,L+1)} \frac{\left| \sum_{\varkappa} \sqrt{2\,j+1}\; Q_{\varkappa \varkappa_i}(\pi L) \right|^2}{\sum_{\varkappa} |\, Q_{\varkappa \varkappa_i}(\pi L)\,|^2}. \tag{30}$$

Correspondingly we obtain an expression for $j_i = 3/2$, that is for the L_{III}, M_{III}, M_{IV} subshell by help of Eq. (A 30).

$$b_k(\pi L, \pi L) = 1 + \frac{k\,(k+1)}{2\,L\,(L+1) - k\,(k+1)} \left[c_1(\pi L) + \frac{k\,(k+1) - 3\,L\,(L+1)}{(L-1)\,(L+2)}\, c_2(\pi L) \right] \tag{31}$$

with

$$c_1(\pi L) = \frac{\left| \sum_{\varkappa} \sqrt{2\,j+1} \begin{pmatrix} L & j & {}^3/_2 \\ 0 & -{}^1/_2 & {}^1/_2 \end{pmatrix} Q_{\varkappa \varkappa_i}(\pi L) \right|^2}{\sum_{\varkappa} |\, Q_{\varkappa \varkappa_i}(\pi L)\,|^2}$$

and

$$c_2(\pi L) = \frac{\left| \sum_{\varkappa} \sqrt{2\,j+1} \begin{pmatrix} j & L & {}^3/_2 \\ {}^1/_2 & -2 & {}^3/_2 \end{pmatrix} Q_{\varkappa \varkappa_i}(\pi L) \right|^2}{\sum_{\varkappa} |\, Q_{\varkappa \varkappa_i}(\pi L)\,|^2}.$$

The second term cancels for dipole transitions i.e. $c_2(\pi\, 1) = 0$.

Considering the particle parameter for *mixed multipole* transitions, i.e. $L = L' \pm 1$, and restricting ourselves first of all to $j_i = {}^1/_2$, that is to the K, L_I, L_{II}, M_I, M_{II} subshells, the particle parameter $b_K\,(\pi L, \pi L')$ is independent of the tensor parameter k, as can be seen by inserting Eq. (A 29) in eq.

$$b_k(\pi L, \pi' L') = \frac{-1}{\sqrt{(2\,L+1)\,(2\,L'+1)}} \times \frac{Re\left\{ \sum_{\varkappa} (-)^{\varkappa} \sqrt{2\,L - |\,\varkappa\,| + 1}\; Q_{\varkappa \varkappa_i}(\pi L) \sum_{\varkappa'} (-)^{\varkappa'} \sqrt{2\,L' - |\,\varkappa'\,| + 1}\; Q_{\varkappa' \varkappa_i}(\pi' L') \right\}}{\sqrt{\sum_{\varkappa} |\, Q_{\varkappa \varkappa_i}(\pi L)\,|^2 \sum_{\varkappa'} |\, Q_{\varkappa' \varkappa_i}(\pi' L')\,|^2}}. \tag{32}$$

The mixed particle parameters for the L_{III}, M_{III} and M_{IV} shells, that is for $j_i = {}^3/_2$, can be reduced by means of Eq. (A 31) and is given by

$$b_k(\pi L, \pi' L') = \bar{c}_1 + k\,(k+1)\,\bar{c}_2 \tag{33}$$

with

$$\bar{c}_i = \frac{Re\left\{ \sum_{\varkappa \varkappa'} C^{(i)}_{(j\, j')} \sqrt{(2\,j+1)\,(2\,j'+1)}\; Q_{\varkappa \varkappa_i}(\pi L)\, Q^{+}_{\varkappa' \varkappa_i}(\pi' L') \right\}}{\sqrt{\sum_{\varkappa} |\, Q_{\varkappa \varkappa_i}(\pi L)\,|^2 \sum_{\varkappa} |\, Q_{\varkappa \varkappa_i}(\pi' L')\,|^2}}.$$

The coefficients $C^{(i)}(j\,j')$ are combinations of $3j$-symbols and are defined in the appendix, Eqs. (A 31) and (A 32).

Similar relations could be derived for higher subshells, i.e. $j_i = 5/2,\ 7/2$. In these cases it is more economic, however, to use the general formula (29), directly. It should be mentioned that similar formulas as Eqs. (30) and (32) have been given by BIEDENHARN and ROSE [9, 10]. The particle parameters for mixed multipoles (Eqs. 32 and 33) carry the correct sign.

Reduced Matrix Elements in Terms of radial Integrals

The evaluation of the reduced matrix elements as defined in Eq. (23) amounts to the computation of the conversion matrix elements as defined in Eqs. (12) and (19). Let us start with the magnetic amplitudes, defined as

$$\langle \varkappa\,\mu \mid M_{L\,M}(M) \mid \varkappa_i\,\mu_i\rangle = \langle \varkappa\,\mu \mid M^{(s)}_{L\,M}(M) + M^{(d)}_{L\,M}(M) \mid \varkappa_i\,\mu_i\rangle\,.$$

We shall content ourselves with the static matrix element, since both static and dynamic terms have the same angular dependence. We insert in Eq. (12) the nuclear transition current

$$\boldsymbol{j}_e = \psi_f\,\boldsymbol{\alpha}\,\psi_i\,.$$

The electronic charge e is omitted and already contained in the overall factor of the general particle parameter. With Eq. (A 2) we obtain

$$\langle \varkappa\mu \mid M_{L\,M}(M) \mid \varkappa_i\,\mu_i\rangle = \frac{1}{\sqrt{L\,(L+1)}}\left\{\langle \Phi^{\mu}_{\varkappa} \mid \boldsymbol{\sigma}\,\boldsymbol{L}\,i^L\,Y_{L\,M} \mid -\,S(\varkappa_i)\,\Phi^{\mu_i}_{-\varkappa_i}\rangle \int_0^\infty dr\,h_L\,u_{\varkappa}\,v_{\varkappa_i}\right.$$
$$\left. +\,\langle -\,S(\varkappa)\,\Phi^{\mu}_{-\varkappa} \mid \boldsymbol{\sigma}\,\boldsymbol{L}\,i^L\,Y_{L\,M} \mid \Phi^{\mu_i}_{\varkappa_i}\rangle \int_0^\infty dr\,h_L\,u_{\varkappa_i}\,v_{\varkappa}\right\}.$$

The angular matrix element may be integrated by parts by means of

$$\boldsymbol{\sigma}(\boldsymbol{L}\,i^L\,Y_{L\,M})\,\Phi^{\mu_i}_{\varkappa_i} = (\boldsymbol{\sigma}\,\boldsymbol{L})\,(i^L\,Y_{L\,M}\,\Phi^{\mu_i}_{\varkappa_i}) - i^L\,Y_{L\,M}\,\boldsymbol{\sigma}\,\boldsymbol{L}\,\Phi^{\mu_i}_{\varkappa_i}$$

and, thus

$$\langle \varkappa\,\mu \mid M^{(s)}_{L\,M}(M) \mid \varkappa_i\,\mu_i\rangle = \frac{-\,S(\varkappa)\,(\varkappa+\varkappa_i)}{\sqrt{L\,(L+1)}}\,\langle \Phi^{\mu}_{-\varkappa} \mid i^L\,Y_{L\,M} \mid \Phi^{\mu_i}_{\varkappa_i}\rangle\,R_{\varkappa\varkappa_i}(M\,L)$$

with

$$R_{\varkappa\varkappa_i}(M\,L) = \int_0^\infty dr\,h_L(k\,r)\,(u_{\varkappa_i}\,v_{\varkappa} + v_{\varkappa_i}\,u_{\varkappa})\,.$$

The angular matrix element still contains all selection rules.

The explicit evaluation in terms of $3j$-symbols, Eq. (A 9) leads to

$$\langle \varkappa\,\mu \mid M^{(s)}_{L\,M}(M) \mid \varkappa_i\,\mu_i\rangle = (-)^{j-\mu}\begin{pmatrix} j_i & L & j \\ \mu_i & M & -\mu \end{pmatrix}(-)^{j+1/2}\,i^{l_i+L-\bar{l}}\,S(\varkappa)\,(\varkappa+\varkappa_i)$$
$$\times\sqrt{\frac{(2\,L+1)\,(2\,j+1)\,(2\,j_i+1)}{4\,\pi\,L\,(L+1)}}\begin{pmatrix} j_i & j & L \\ 1/2 & -1/2 & 0 \end{pmatrix} R_{\varkappa\varkappa_i}(M\,L)\,.$$

For the dynamic matrix element we obtain the same result except that the radial integral $R_{\varkappa\varkappa_i}$ is replaced by

$$T_{\varkappa\varkappa_i}(M\,L) = \frac{\int_0^\infty d\tau_n \boldsymbol{j}_n \boldsymbol{L}\, g^{(3)}_{\varkappa\varkappa_i}(r)\ (i^L\ Y_{LM})^+}{\int_0^\infty d\tau_n \boldsymbol{j}_n \boldsymbol{L}\, j_L(k\,r)\ (i^L\ Y_{LM})^+} \tag{34}$$

with

$$g^{(3)}_{\varkappa\varkappa_i}(r) = h_L(k\,r)\int_0^r dr\, j_L(k\,r)\,(u_{\varkappa_i} v_\varkappa + v_{\varkappa_i} u_\varkappa) - j_L(k\,r)\int_0^r dr\, h_L(k\,r)\,(u_{\varkappa_i} v_\varkappa + v_{\varkappa_i} u_\varkappa)\,. \tag{35}$$

Finally we get for the reduced matrix element

$$\langle\varkappa \parallel ML \parallel \varkappa_i\rangle = (-)^{j+1/2}\, i^{l_i+L-l}\, S(\varkappa)\,(\varkappa_i+\varkappa)\sqrt{\frac{(2L+1)\,2j+1)\,(2j_i+1)}{4\pi L\,(L+1)}}\begin{pmatrix} j_i & j & L \\ 1/2 & -1/2 & 0\end{pmatrix}$$
$$\times\,[R_{\varkappa\varkappa_i}(M\,L) + T_{\varkappa\varkappa_i}(M\,L)]\,. \tag{36}$$

For electric transitions the procedure is quite analogous and again we shall consider only the static part.

$$\langle\varkappa\,\mu \mid M^{(s)}_{LM}(M) \mid \varkappa_i\,\mu_i\rangle = \frac{1}{\sqrt{L\,(L+1)}}\int_0^\infty \left(i\,k\,\boldsymbol{j}_e\,\boldsymbol{r} - \varrho\,\frac{\partial}{\partial r}\,r\right) h_L(k\,r)\,i^L\,Y_{LM}\,d\tau\,.$$

The transition charge density ϱ_e is defined as

$$\varrho_e = \psi_f^+\,\psi_i$$

and thus we get by use of Eq. (A 6) in the appendix

$$\langle\varkappa\,\mu \mid M^{(s)}_{LM}(E) \mid \varkappa_i\,\mu_i\rangle = \frac{1}{\sqrt{L\,(L+1)}}\,\langle\Phi^\mu_\varkappa \mid i^L\,Y_{LM} \mid \Phi^{\mu_i}_{\varkappa_i}\rangle\,R_{\varkappa\varkappa_i}(E\,L)$$

with

$$R_{\varkappa\varkappa_i}(E\,L) = \int_0^\infty dr\left\{k\,r\,h_L(k\,r)\,[u_{\varkappa_i} v_\varkappa - v_{\varkappa_i} u_\varkappa] + \left(\frac{\partial}{\partial r}\,r\,h_L(k\,r)\right)[u_{\varkappa_i} u_\varkappa + v_{\varkappa_i} v_\varkappa]\right\}.$$

Inserting Eq. (A 6) we have

$$\langle\varkappa\,\mu \mid M^{(s)}_{LM}(E) \mid \varkappa_i\,\mu_i\rangle = (-)^{j-\mu}\begin{pmatrix} j_i & L & j \\ \mu_i & M & -\mu\end{pmatrix}(-)^{j+1/2}\,i^{l_i+L-l}\sqrt{\frac{(2L+1)\,(2j+1)\,(2j_i+1)}{4\pi L\,(L+1)}}$$
$$\times\begin{pmatrix} j_i & j & L \\ 1/2 & -1/2 & 0\end{pmatrix} R_{\varkappa\varkappa_i}(E\,L)\,.$$

In the dynamic matrix element the radial integral $R_{\varkappa\varkappa_i}$ is replaced by

$$T_{\varkappa\varkappa_i}(E\,L) = \frac{\int_0^\infty d\tau\,\{i\,\boldsymbol{j}_n\,\hat{r}\,g^{(1)}_{\varkappa\varkappa_i}(r) + \varrho_n\,g^{(2)}_{\varkappa\varkappa_i}(r)\}\,(i^L\,Y_{LM})^+}{\int_0^\infty d\tau\left\{i\,\boldsymbol{j}_n\,\hat{r}\,k\,r\,j_L(k\,r) + \varrho\,\frac{\partial}{\partial r}\,r\,j_L(k\,r)\right\}(i^L\,Y_{LM})^+} \tag{37}$$

with

$$g^{(1)}_{\varkappa\varkappa_i}(r) = -\frac{i}{k}\,(u_{\varkappa_i}\,v_\varkappa - v_{\varkappa_i}\,u_\varkappa) + k\,r\,\{h_L\,f(r, j_L) - j_L\,f(r, h_L)\}$$

$$g^{(2)}_{\varkappa\varkappa_i}(r) = \left(\frac{\partial}{\partial r}\,r\,h_L(k\,r)\right) f(r, j_L) - \left(\frac{\partial}{\partial r}\,r\,j_L(k\,r)\right) f(r, h_L)$$

$$f(r, \xi_L) = \int_0^r dr\left\{k\,r\,\xi_L\,(u_{\varkappa_i}\,v_\varkappa - v_{\varkappa_i}\,u_\varkappa) + \frac{\partial}{\partial r}\,r\,\xi_L\,(u_{\varkappa_i}\,u_\varkappa + v_{\varkappa_i}\,v_\varkappa)\right\}. \qquad (38)$$

Finally we obtain the reduced matrix element for electric transitions

$$\langle\varkappa \parallel E\,L \parallel \varkappa_i\rangle = (-)^{j-1/2}\,i^{l_i+L-l}\sqrt{\frac{(2\,L+1)\,(2\,j+1)\,(2\,j_i+1)}{4\,\pi\,L\,(L+1)}}\begin{pmatrix} j_i & j & L \\ 1/2 & -1/2 & 0\end{pmatrix}[R_{\varkappa\varkappa_i}(E\,L) + T_{\varkappa\varkappa_i}(E\,L)]\,. \qquad (39)$$

Together with Eqs. (37) and (39) the conversion coefficient can be written in terms of radial integrals for electric transitions

$$\alpha_L(\varkappa_i) = \pi\,\alpha\,k\sum_\varkappa \frac{(2\,j_i+1)\,2\,j+1)}{L\,(L+1)}\begin{pmatrix} j_i & j & L \\ 1/2 & -1/2 & 0\end{pmatrix}^2 |\,R_{\varkappa\varkappa_i}(EL) + T_{\varkappa\varkappa_i}(E\,L)\,|^2 \qquad (40a)$$

and for magnetic transitions

$$\beta_L(\varkappa_i) = \pi\,\alpha\,k\sum_\varkappa \frac{(2\,j_i+1)\,(2\,j+1)}{L\,(L+1)}\begin{pmatrix} j_i & j & L \\ 1/2 & -1/2 & 0\end{pmatrix}^2 (\varkappa+\varkappa_i)^2\,|\,R_{\varkappa\varkappa_i}(M\,L) + T_{\varkappa\varkappa_i}(M\,L)\,|^2 \qquad (40b)$$

IV. Further Investigation of the Dynamic Matrix Elements

In this chapter we shall discuss only the dynamic matrix element $T_{\varkappa\varkappa_i}$ which is defined in Eqs. (34) and (35) for magnetic transitions and in Eqs. (37) and (38) for electric transitions.

In the expression of T the nominator and denominator is described by the same nuclear transition operators which are, however, weighted by different radial functions, and it is possible to obtain information on dynamic nuclear properties through the internal conversion process. In general, however, the nuclear contribution to the internal conversion will be small and outside the present experimental limits of error. Only in those cases where the gamma transition is hindered, while the conversion is unhindered, dynamic nuclear effects may be expected. Especially in E1 and M1 transitions many anomalies were observed which can be explained by dynamic or penetration effects. It should be noted that anomalies may occur also in higher order multipole transitions.

Let us assume that the nucleus is a homogenously charged sphere with sharp edge. The radius of this sphere can be assumed to be

$$R = 1.20\,A^{1/3}\,10^{-13}\text{ cm} = 0.00311\,A^{1/3}\,\lambda\!\!\!^{-}_c\,.$$

Inside the nucleus, the argument $k\,r$ of the spherical Bessel or Hankel functions is small compared to one, i.e. $k\,r \ll 1$. We may therefore restrict ourselves to the first term of the series expansion,

i.e.

$$j_L(k\,r) = \frac{(k\,r)^L}{(2\,L+1)!!} \qquad h_L(k\,r) = -i\,\frac{(2\,L-1)!!}{(k\,R)^{L+1}}\,.$$

The Coulomb functions and similarly the radial functions $g^{(j)}_{\varkappa\,\varkappa_i}(r)$ may be expanded into a power series of $x = r/R$ [20], i.e.

$$g^{(1)}_{\varkappa\,\varkappa_i}(r) = i\,\frac{x^p}{k}\sum_{m=0}^{\infty} d_m\,x^{2\,m} \qquad g^{(2)}_{\varkappa\,\varkappa_i}(r) = i\,\frac{x^{\bar p}}{k}\sum_{m=0}^{\infty} e_m\,x^{2\,m} \tag{41}$$

and

$$g^{(3)}_{\varkappa\,\varkappa_i}(r) = i\,\frac{x^p}{k}\sum_{m=0}^{\infty} f_m\,x^{2m}$$

with

$$p = \begin{matrix}|\,\varkappa_i\,| + |\,\varkappa\,| + 1\\ |\,\varkappa_i\,| + |\,\varkappa\,|\end{matrix} \qquad \bar p = \begin{matrix}|\,\varkappa_i\,| + |\,\varkappa\,|\\ |\,\varkappa_i\,| + |\,\varkappa\,| + 1\end{matrix} \qquad \text{for} \begin{matrix}\varkappa\,\varkappa_i > 0\\ \varkappa\,\varkappa_i < 0\,.\end{matrix}$$

The dynamic matrix elements can now be written

$$T_{\varkappa\,\varkappa_i}(E\,L) = i\,\frac{(2\,L+1)!!}{(L+1)}\,\frac{1}{k\,(k\,R)^L}\,\frac{1}{(1+c)}\sum_{m=0}^{\infty} d_m\,\eta_m^{(p)} + e_m\,\xi_m^{(\bar p)}$$

$$T_{\varkappa\,\varkappa_i}(M\,L) = i\,(2\,L+1)!!\,\frac{1}{k\,(k\,R)^L}\sum_{m=0}^{\infty} f_m\,\lambda_m^{(p)}$$

where

$$\eta_m^{(p)} = \frac{\langle I_f \,\|\, i\,\boldsymbol{j}_n\,\hat{\boldsymbol{r}}\,x^{p+2\,m}\,Y_L \,\|\, I_i\rangle}{\langle I_f \,\|\, \varrho_n\,x^L\,Y_L \,\|\, I_i\rangle} \qquad c = \frac{k\,R}{L+1}\,\eta_0^{(L+1)}$$

$$\xi_m^{(\bar p)} = \frac{\langle I_f \,\|\, \varrho_n\,x^{\bar p+2\,m}\,Y_L \,\|\, I_i\rangle}{\langle I_f \,\|\, \varrho_n\,x^L\,Y_L \,\|\, I_i\rangle} \qquad \lambda_m^{(p)} = \frac{\langle I_f \,\|\, \boldsymbol{j}_n\,\boldsymbol{L}\,x^{p+2\,m}\,Y_L \,\|\, I_i\rangle}{\langle I_f \,\|\, \boldsymbol{j}_n\,\boldsymbol{L}\,x^L\,Y_L \,\|\, I_i\rangle}\,. \tag{42}$$

In the above expressions the parameters η_m, ξ_m and λ_m contain all nuclear information and could be evaluated if a specific nuclear model is assumed. The coefficients d_m, e_m and f_m can be calculated exactly for any specific static charge distribution of the nucleus and are given in the appendix for our used charge distribution. As long as we deal only with small energies, the assumption of a sharp edged sphere seems to be reasonable and the introduction of a more physical charge distribution would not change these coefficients appreciably [3].

In Table 1 we give the Dirac quantum number $\varkappa$, the quantities p, $\bar p$ and $q = |\,\varkappa_i\,| + |\,\varkappa\,|$ (see Eq. (37)) for all possibilities of the ejected electron. The dynamic matrix element $T_{\varkappa\,\varkappa_i}$ is proportional to the product of the normalization coefficients of the bound and continuum states, i.e. $T_{\varkappa\,\varkappa_i} \sim a_0 A_0 \sim R^q$. For a definite multipole transition L the partial wave with the lowest value of $|\,\varkappa\,|$ is characterized by $q = L + 1$. The corresponding matrix element is therefore about a factor 100 larger compared to the others, which we will neglect in the following. The number of model independent nuclear parameter can be further reduced.

We consider first for magnetic multipole transitions the ratio

$$F_m = \frac{f_m}{f_0}$$

which do not depend on the normalization coefficients and thus can be computed directly by means of Eq. (A 21).

Table 1

Selection rules for the outgoing electron ($\varkappa$) in dependence on the multipolarity L for electric (left) and magnetic (right) transitions. Simultaneously, the values of p, $\bar{p}$ and q are given.

$\varkappa_i$	$\varkappa$	p	q
-1	$-L$	$L+2$	$L+1$
	$L+1$	$L+2$	$L+2$
-2	$-(L-1)$	$L+2$	$L+1$
	L	$L+2$	$L+2$
	$-(L+1)$	$L+4$	$L+3$
	$L+2$	$L+4$	$L+4$
-3	$-(L-2)$	$L+2$	$L+1$
	$L-1$	$L+2$	$L+2$
	$-L$	$L+4$	$L+3$
	$L+1$	$L+4$	$L+4$
	$-(L+2)$	$L+6$	$L+5$
	$L+3$	$L+6$	$L+6$

$\varkappa_i$	$\varkappa$	p	$\bar{p}$	q
-1	L	$L+1$	$L+2$	$L+1$
	$-(L+1)$	$L+3$	$L+2$	$L+2$
-2	$L-1$	$L+1$	$L+2$	$L+1$
	$-L$	$L+3$	$L+2$	$L+2$
	$L+1$	$L+3$	$L+4$	$L+3$
	$-(L+2)$	$L+5$	$L+4$	$L+4$
-3	$L-2$	$L+1$	$L+2$	$L+1$
	$-(L-1)$	$L+3$	$L+2$	$L+2$
	L	$L+3$	$L+4$	$L+3$
	$-(L+1)$	$L+5$	$L+4$	$L+4$
	$L+2$	$L+5$	$L+6$	$L+5$
	$-(L+3)$	$L+7$	$L+6$	$L+6$

We define now a nuclear parameter λ, independent of any subshell, by

$$\lambda = \lambda_0^{(L+1)} + F_1 \lambda_1^{(L+1)} + F_2 \lambda_2^{(L+1)} + \cdots \tag{43}$$

where $\lambda_i^{(L+1)}$ is defined in Eq. (42). The number of nuclear parameters in magnetic transitions is thus reduced to one, which contains all nuclear information and which has to be consistent with all conversion data of a distinct nuclear ML transition. The dynamic matrix element can now finally be written

$$T_{\varkappa\varkappa_i}(M\,L) = i\,\frac{(2\,L+1)!!}{k\,(k\,R)^L}\,f_0(\varkappa, \varkappa_i)\,\lambda\,\delta_{q,\,L+1}\,. \tag{44}$$

For electric multipole transitions the same arguments as in the magnetic transitions are valid and we define corresponding to Eqs. (40), (41) and (42) for all electric multipole ordess (except electric dipole transitions)

$$\eta = \frac{1}{1+c}\,(\eta_0^{(L+1)} + D_1\,\eta_1^{(L+1)} + D_2\,\eta_2^{(L+1)} + \cdots)$$

$$\xi = \frac{1}{1+c}\,(\xi_0^{(L+2)} + E_1\,\xi_1^{(L+2)} + E_2\,\xi_2^{(L+2)} + \cdots)$$

$$D_m = \frac{d_m}{d_0}\,; \qquad E_m = \frac{e_m}{e_0}\,. \tag{45}$$

For the dynamic matrix element we get finally

$$T_{\varkappa\varkappa_i}(E\,L) = i\,\frac{(2\,L+1)!!}{k(kR)^L\,(L+1)}\,(d_0(\varkappa, \varkappa_i)\,\eta + e_0(\varkappa, \varkappa_i)\,\xi)\,\delta_{q,\,L+1}\,. \tag{46}$$

The "nuclear current parameter" η as well as the "nuclear charge parameter" ξ does not depend on the subshell. – For electric dipole ($E1$) transitions, a strong cancellation occurs in the dynamic coefficients of ξ. Thus, the $q = L + 1 = 2$ term is no longer the leading term and we have to include matrix elements with $q = 3$. We restrict in this case ourselves in Eq. (38) to the first term with $m = 0$ and redefine the nuclear charge parameter:

$$\xi = \frac{1}{1+c}\,\xi_0^{(L+2)} \tag{47}$$

the dynamic matrix elements can now be written

$$T_{\varkappa\varkappa_i}(E\,1) = i\,\frac{3}{2\,R\,k^2}\,[d_0\,\eta\,\delta_{q,2} + (e_0\,\delta_{q,2} + e_0\,\delta_{q,3})\,\xi]\,. \tag{48}$$

The restriction to the first term in the series expansion is necessary, since the coefficients E_m for $q = 2$ are not the same ones as for $q = 3$. However, the charge parameter is not very important, and experimentally it is in most cases even consistent with zero.

The above approximation i.e. the neglection of the dynamic matrix elements of the higher partial waves, is only true, if

$$\frac{\nu_{i+1}}{\nu_i} \lesssim 10 \tag{49}$$

where ν_i is one of the nuclear parameters (η_i, ξ_i or λ_i).

This condition is, however, rather weak and will be fulfilled in general.

We like to stress that, as long as the condition (49) holds the discussed neglections will have little influence on the numerical values. The above equations of the dynamic matrix elements must thus be regarded as exact relations.

Similar, but less general parametrizations have been given earlier in the literature. In Table 2 we give a comparison between the present and the corresponding notation of earlier authors [3, 6, 21].

Table 2

Different notations of the nuclear parameters. The present parameters are expressed in the notation of other authors.

Present	Corresponding notation of earlier authors	Reference	Remarks
$\frac{\eta_0^{(L+1)}}{1+c}\left(1+\frac{s_1^{(1)}}{s_0^{(1)}}\frac{\eta_1^{(L+1)}}{\eta_0^{(L+1)}}\right)$	$(1+\sigma_j'')\sqrt{\frac{L+1}{L}}\,k\,R\,\lambda_j''$	CHURCH and WENESER [3]	Defined in [3] for the K-shell and correct for $j = L-{}^1/_2$, only.
$\frac{\xi_0^{(L+2)}}{1+c}\left(1+\frac{s_1^{(2)}}{S_0^{(2)}}\frac{\xi_1^{(L+2)}}{\xi_0^{(L+2)}}\right)$	$(1+\sigma_j')\sqrt{\frac{L+1}{L}}\,\lambda_j'$		Church and Weneser give also the relation to the notation of GREEN and ROSE [4]
$\frac{\eta_0^{(2)}}{1+c}$	$-\frac{2}{B\,R}\sqrt{\frac{1}{3\,\pi\,\alpha}}\,Y$	EMERY and PERLMAN [21]	only for $E1$
$\frac{\xi_0^{(3)}}{1+c}$	$\frac{1}{R^2}\sqrt{\frac{3}{\pi\,\alpha}}\,X$		
$\frac{\eta_m^{(2)}}{1+c}$ $m = 0, 1, 2, \ldots$	$-\frac{2}{3}\,\lambda s$, $s = 0, 2, 4, \ldots$	KRAMERS and NILSSON [6]	only for $E1$
λ	λ	CHURCH and WENESER [3]	

We can separate the conversion coefficient into a static part depending only on the electron wave functions and an "anomaly factor" $\Delta(\sigma)$, which contains all nuclear

information. For a specific subshell σ, the conversion coefficient for magnetic transition of multipolarity L can be written

$$\beta_L(\sigma) = \beta_L^{(0)}(\sigma)\, \Delta(\sigma) \tag{50}$$

with

$$\Delta(\sigma) = 1 + b_1(\sigma)\, \lambda + b_2(\sigma)\, \lambda^2$$

where $\beta_L^{(0)}(\sigma)$ is the "static conversion coefficient". In the approximation of ROSE, all penetration effects are neglected, i.e. $\lambda = 0$ and $\Delta = 1$. The surface model of SLIV et al. assumes the value $\lambda_i = 1$ for the nuclear parameter.

A corresponding anomaly factor $\overline{\Delta}(\sigma)$ can be defined for the particle parameters of the subshell, i.e.

$$b_k(\sigma) = b_k^{(0)}(\sigma)\, \overline{\Delta}(\sigma) \quad \text{with} \quad \overline{\Delta}(\sigma) = \frac{\Gamma(\sigma)}{\Delta(\sigma)} \tag{51a}$$

where $\Delta(\sigma)$ is given by Eq. (50) and Γ by

$$\Gamma(\sigma) = 1 + c_1(\sigma)\, \lambda + c_2(\sigma)\, \lambda^2 \tag{51b}$$

The conversion coefficient for an electric multipole transition can be factorized in a similar way into a static part $\alpha_L^{(0)}(\sigma)$ and a dynamic part, the anomaly factor $\Delta(\sigma)$.

$$\alpha_L(\sigma) = \alpha_L^{(0)}(\sigma)\, \Delta(\sigma) \tag{52a}$$

with

$$\Delta(\sigma) = 1 + a_1(\sigma)\, \eta + a_2(\sigma)\, \eta^2 + a_3(\sigma)\, \eta\xi + a_4(\sigma)\, \xi + a_5(\sigma)\, \xi^2 . \tag{52b}$$

For the particle parameters of electric multipole transitions the anomaly factor $\Gamma(\sigma)$ (Eq. 51a) is replaced by

$$\Gamma(\sigma) = 1 + c_1(\sigma)\, \eta + c_2(\sigma)\, \eta^2 + c_3(\sigma)\, \eta\xi + c_4(\sigma)\, \xi + c_5(\sigma)\, \xi^2 . \tag{53}$$

The nonpenetration model of Rose, corresponds again to $\eta_i = \xi_i = 0$ i.e. $\Delta(\sigma) \equiv 1$, while the connection with SLIV's surface model is given by $\eta_i = 0$ and $\xi_i = 1$. Since the coefficients $a_4(\sigma)$ and $a_5(\sigma)$ are usually much smaller than one, $\Delta(\sigma) \equiv 1$ is also an admittable approximation for electric multipoles, in SLIV's model.

V. Numerical Results and Discussion

Today, two tabulations of the internal conversion coefficients are available, i.e. those of ROSE [13] and those of SLIV [14]. Both authors include the screening of the atomic electrons by the Thomas-Fermi-Dirac model as well as finite nuclear size corrections, although the latter in a somewhat different manner. It is known, that the two tabulations differ by larger amounts than could be understood by their different inclusion of finite size effects. In order to check the results of ROSE and SLIV we have performed a recalculation of the internal conversion matrix elements and phases. In the following we shall give an outline of our numerical procedure.

1. *Numerical procedure*

The eigenvalues and eigenfunctions of the bound states were found with the help of a method described by ROSE [16] which we reproduce in outline in the following.

As an approximate eigenvalue we choose $W = 1 - \varepsilon_q/m_c c^2$ where ε_q represents the binding energy of the electron. This values have been recently tabulated by HAGSTRÖM et al. [22]. The Dirac equation was solved numerically from the origin up to a matching point r_0 and the left side ratio $\varrho_L(r_0) = (v_{xi}/u_{xi})_{r=r_0}$ was computed.

Then, we choose a point $r_1 \gg r_0$, where the asymptotic solutions [16] are exact up to a relative error of about 10^{-4}. The Dirac equation was solved numerically for $r < r_1$ and the right side ratio $\varrho_R(r_0) = (v_{xi}/u_{xi})_{r=r_0}$ at the matching point r_0 was computed.

The correct eigenvalue is defined by the relation $\varrho_R = \varrho_L$ at the matching point. If this condition is not fulfilled a corrector formula leads to a better eigenvalue. With the corrected eigenvalue the above procedure was repeated. As soon as the absolute value of

$$\chi = \frac{\varrho_R(r_0)}{\varrho_L(r_0)} - 1$$

was less than 10^{-4}, the iteration was stopped. It should be mentioned, that because of numerical instabilities the numerical solutions are very sensitive to the matching point r_0. We have obtained the most exact results choosing the matching point to be a little smaller than the classical turning point. We have also checked the normalized wave functions for a point nucleus of the K- and L-subshell with the pure Coulomb wave function. The agreement within 10^{-4} was better than over about 600 compton wave lengths.

For the normalization of the continuum wave functions we use the following method. For $V \equiv 0$, the regular solutions of the Dirac equation are given by [20]

$$u_\varkappa^{(0)} = \sqrt{\frac{W+1}{\pi p}}\, p r\, j_l(p r) \qquad v_\varkappa^{(0)} = S(\varkappa) \sqrt{\frac{W-1}{\pi p}}\, p r\, j_{\bar{l}}(p r) \tag{54}$$

and the irregular solutions by

$$\bar{u}_\varkappa^{(0)} = \sqrt{\frac{W+1}{\pi p}}\, p r\, n_l(p r) \qquad \bar{v}_\varkappa^{(0)} = S(\varkappa) \sqrt{\frac{W-1}{\pi p}}\, p r\, n_{\bar{l}}(p r)\,. \tag{55}$$

In the above equations, p is the momentum and $l(\varkappa)$ is the "orbital angular momentum" of the electron. The spherical Neumann functions are denoted by n_l. The asymptotic behaviour of those solutions are discussed in (A 11). The general solution of the Dirac equation for a zero potential is a combination of the regular and irregular solutions. These equations and the asymptotic behaviour are sufficient to determine the normalization and the phases of the partial waves. Since the actual potential vanishes for large distances, the actual numerical wave functions will approach the $Z = 0$ limit, i.e.

$$u_\varkappa = a\, u_\varkappa^{(0)} + b\, \bar{u}_\varkappa^{(0)} \qquad v_\varkappa = a\, v_\varkappa^{(0)} + b\, \bar{v}_\varkappa^{(0)}\,. \tag{56}$$

We investigated the behaviour of the coefficients a and b in Eq. (56) and did not compare the actual wave functions with the free particle or with the asymptotic solutions. This method was found to converge rapidly. As soon as a and b were constant within $3 \cdot 10^{-3}$ over two wavelengths, the integration was stopped and the normalization factor as well as the phase averaged over one wavelength. The numerical error of about 1% of our conversion coefficients arises mainly from the relatively large

error in the normalization of the continuum states and could be reduced easily by the use of more computer time.

For the integration of the differential equations both, the Runge-Kutta and the Adams-Moulton-Bashfort scheme [23] have been used. In the final calculations the latter method has been preferred saving computer time. We have checked finally our programs by the calculation of the conversion coefficients for a pure Coulomb potential [1]. We found agreement within the estimated limit of error.

In our calculations screening was taken into account by the Thomas-Fermi-Dirac model [24]. We used the same screening function for the bound states as well as for the continuum states. By reasons of consistency, we have not included the hole as introduced by ROSE [13], especially since this hole would not change the conversion coefficients by more than $^1/_2$ percent, even in medium heavy nuclei.

2. *Numerical results*

The conversion coefficients in SLIV's and ROSE's tables differ by rather large amounts [25] which cannot be only due to their different handling of the penetration effects. Thus, numerical inconsistencies may exist in one or both of the tables. A possible explanation for these deviations was given by BHALLA et al. [26] pointing out that the interpolated conversion coefficients fluctuate around a smooth curve of calculated values and that the use of the eight-point interpolation formula may be responsible for these fluctuations. In order to check the calculated results of SLIV and to exclude these interpolation errors we have recalculated some L-subshell conversion coefficients and particle parameters at the same point as in SLIV's tables. The errors of interpolation are still contained in the comparison with Rose's values. The results of this recalculation are given in Tables 3–8.

A more concentrated and illustrative comparison is shown in figure 1 for electric transitions. The values of ROSE are compared with our static conversion coefficients (i.e. $\Delta \equiv 1$, see chapter IV) by computing the quantity

$$R = \frac{\alpha_{L,\,\mathrm{Rose}}}{\alpha_L^{(0)}(\sigma)} .$$

SLIV's values are compared with our values for the surface model (SM) (i.e. $\eta = 0$ and $\xi_i = 1$, see chapter IV), i.e.

$$S = \frac{\alpha_{L,\,\mathrm{Sliv}}}{\alpha_L(\sigma)_{SM}} .$$

ROSE and SLIV estimate their computational error to be about 2%. SLIV suggests that the error may pass over this limit for smaller Z and higher energies. Except some coefficients in these areas we agree with SLIV's values within the combined limits of error. As expected the agreement with ROSE's calculation is better for larger energies and smaller Z. Particular exceptions may be due to the above mentioned interpolation uncertainty. The similar behaviour occurs in the comparison of the conversion coefficients for magnetic transitions (see Figure 2). We have plotted the quantities

$$R = \frac{\beta_{L,\,\mathrm{Rose}}}{\beta_L^{(0)}(\sigma)}$$

and

$$S = \frac{\beta_{L,\,\mathrm{Sliv}}}{\beta_L(\sigma)_{SM}} .$$

Table 3

The results of our recalculation for electric dipole ($E1$) transition. The static conversion coefficients are presented together with the dynamic coefficients for the energies $k = 0.1$ and $k = 1.0$ ($m_e c^2$). The results of ROSE and of SLIV are given in columns 1 and 2 respectively.

k ($m_e c^2$)	σ	Z	ROSE [13] α_1	SLIV [14] α_1	$\alpha_1^{(0)}(\sigma)$	$a_1(\sigma)$	$a_2(\sigma)$	$a_3(\sigma)$	$a_4(\sigma)$	$a_5(\sigma)$
0.1	L_{I}	61	.118(0)	.123(0)	.123(0)	−.528(−1)	.273(−2)	.884(−5)	−.303(−3)	.231(−7)
		69	.139(0)	.145(0)	.145(0)	−.990(−1)	.950(−2)	.327(−4)	−.571(−3)	.825(−7)
		81	.154(0)	.171(0)	.170(0)	−.265(0)	.651(−1)	.237(−3)	−.144(−2)	.530(−6)
		88	.154(0)	.178(0)	.179(0)	−.499(0)	.219(0)	.845(−3)	−.262(−2)	.178(−5)
		95	.136(0)	.180(0)	.181(0)	−.967(0)	.762(0)	.295(−2)	−.462(−2)	.559(−5)
	L_{II}	61	.382(−1)	.399(−1)	.393(−1)	.271(−1)	.368(−2)	−.198(−4)	−.916(−4)	.268(−7)
		69	.607(−1)	.640(−1)	.632(−1)	.429(−1)	.109(−1)	−.629(−4)	−.157(−3)	.906(−7)
		81	.106(0)	.116(0)	.115(0)	.855(−1)	.572(−1)	−.347(−3)	−.340(−3)	.530(−6)
		88	.137(0)	.155(0)	.157(0)	.134(0)	.164(0)	−.105(−2)	−.570(−3)	.168(−5)
		95	.162(0)	.202(0)	.206(0)	.212(0)	.472(0)	−.304(−2)	−.913(−3)	.493(−5)
	L_{III}	61	.537(−1)	.555(−1)	.544(−1)				−.639(−4)	.119(−7)
		69	.810(−1)	.830(−1)	.818(−1)				−.106(−3)	.355(−7)
		81	.136(0)	.136(0)	.134(0)				−.216(−3)	.164(−6)
		88	.172(0)	.173(0)	.172(0)				−.343(−3)	.442(−6)
		95	.212(0)	.214(0)	.212(0)				−.513(−3)	.105(−5)
1.0	L_{I}	61	.380(−3)	.396(−3)	.386(−3)	−.330(−3)	.860(−2)	−.554(−4)	−.694(−3)	.215(−6)
		69	.570(−3)	.581(−3)	.565(−3)	−.577(−3)	.204(−1)	−.140(−3)	−.108(−2)	.544(−6)
		81	.947(−3)	.975(−3)	.949(−3)	−.122(−2)	.775(−1)	−.564(−3)	−.202(−2)	.208(−5)
		88	.130(−2)	.128(−2)	.125(−2)	−.203(−2)	.179(0)	−.137(−2)	−.305(−2)	.506(−5)
		95	.179(−2)	.167(−2)	.164(−2)	−.314(−2)	.418(0)	−.323(−2)	−.435(−2)	.112(−4)
	L_{II}	61	.225(−4)	.267(−4)	.225(−4)	.725(−1)	.148(−1)	−.222(−3)	−.857(−3)	.915(−6)
		69	.459(−4)	.536(−4)	.461(−4)	.985(−1)	.330(−1)	−.530(−3)	−.127(−2)	.221(−5)
		81	.123(−3)	.122(−3)	.122(−3)	.154(0)	.111(0)	−.189(−2)	−.221(−2)	.830(−5)
		88	.207(−3)	.229(−3)	.210(−3)	.205(0)	.241(0)	−.432(−2)	−.319(−2)	.198(−4)
		95	.359(−3)	.371(−3)	.356(−3)	.269(0)	.516(0)	−.932(−2)	−.435(−2)	.431(−4)
	L_{III}	61	.256(−4)	.272(−4)	.255(−4)				−.178(−3)	.102(−6)
		69	.444(−4)	.395(−4)	.441(−4)				−.266(−3)	.169(−6)
		81	.892(−4)	.936(−4)	.889(−4)				−.454(−3)	.526(−6)
		88	.126(−3)	.132(−3)	.126(−3)				−.639(−3)	.118(−5)
		95	.171(−3)	.179(−3)	.175(−3)				−.834(−3)	.240(−5)

Table 4

The results of our recalculation for electric dipole ($E1$) transitions. The static particle parameters $b_2^{(0)}$ are presented together with the dynamic coefficients for the energies $k = 0.1$ and $k = 1.0$ ($m_e c^2$). In column 1 the results of SLIV and BAND (for the L_I- and L_{II}-subshells) and those of MIRANDA et al. (for the L_{III}-subshell) are given.

k ($m_e c^2$)	σ	Z	BAND et al. [29] MIRANDA et al. [30] $b_2(E1)$	$b_2^{(0)}(E1, \sigma)$	$c_1(\sigma)$	$c_2(\sigma)$	$c_3(\sigma)$	$c_4(\sigma)$	$c_5(\sigma)$
0.1	L_I	61	−.195(1)	−.196(1)	−.646(−1)	.421(−5)	.945(−5)	−.306(−3)	.234(−7)
		69	−.194(1)	−.193(1)	−.119(0)	.161(−4)	.321(−4)	−.578(−3)	.832(−7)
		81	−.191(1)	−.190(1)	−.300(0)	.117(−3)	.199(−3)	−.146(−2)	.527(−6)
		88	−.189(1)	−.187(1)	−.536(0)	.408(−3)	.636(−3)	−.266(−2)	.173(−5)
		95	−.187(1)	−.183(1)	−.099(1)	.135(−2)	.195(−2)	−.464(−2)	.526(−5)
	L_{II}	61	−.924(0)	−.955(0)	−.546(−2)	−.375(−8)	−.788(−8)	−.340(−4)	.105(−8)
		69	−.105(1)	−.106(1)	.568(−1)	−.453(−6)	−.857(−6)	−.197(−3)	.274(−8)
		81	−.122(1)	−.123(1)	.280(0)	−.670(−5)	−.109(−4)	−.923(−3)	.345(−7)
		88	−.129(1)	−.128(1)	.610(0)	−.280(−4)	−.416(−4)	−.208(−2)	.137(−6)
		95		−.134(1)	.125(1)	−.103(−3)	−.142(−3)	−.424(−2)	.469(−6)
	L_{III}	61	−.900(0)	−.922(0)				.145(−4)	0
		69	−.108(1)	−.109(1)				−.125(−3)	0
		81	−.133(1)	−.132(1)				−.491(−3)	0
		88	−.145(1)	−.142(1)				−.952(−3)	0
		95	−.155(1)	−.151(1)				−.164(−2)	0
1.0	L_I	61		−.100(1)	−.238(0)	.397(−4)	.877(−4)	.737(−3)	−.161(−6)
		69		−.100(1)	−.353(0)	.106(−3)	.207(−3)	.131(−3)	−.413(−6)
		81		−.100(1)	−.628(0)	.431(−3)	.718(−3)	.260(−3)	−.156(−5)
		88		−.100(1)	−.855(0)	.100(−2)	.154(−2)	.219(−2)	−.351(−5)
		95		−.100(1)	−.118(1)	.223(−2)	.317(−2)	.193(−2)	−.737(−5)
	L_{II}	61		−.216(0)	−.104(0)	.964(−4)	.202(−3)	.696(−2)	−.149(−5)
		69		−.328(0)	−.874(0)	.148(−3)	.276(−3)	.608(−2)	−.206(−5)
		81		−.499(0)	−.721(0)	.304(−3)	.485(−3)	.485(−2)	−.371(−5)
		88		−.598(0)	−.594(0)	.488(−3)	.717(−3)	.360(−2)	−.563(−5)
		95		−.697(0)	−.327(0)	.669(−3)	.914(−3)	.739(−2)	−.688(−5)
	L_{III}	61		.268(0)				−.121(−2)	.632(−7)
		69		.128(0)				−.222(−2)	.539(−7)
		81		.258(−1)				−.148(−1)	.189(−6)
		88		−.787(−1)				.238(−2)	−.433(−7)
		95		−.193(0)				−.184(−2)	−.127(−7)

Table 5

The results of our recalculation for electric quadrupole ($E2$) transition. The static conversion coefficients are presented together with the dynamic coefficients for the energies $k = 0.1$ and $k = 1.0$ ($m_e c^2$). The results of ROSE and of SLIV are given in Columns 1 and 2 respectively.

k ($m_e c^2$)	σ	Z	ROSE [13] α_2	SLIV [14] α_2	$\alpha_2^{(0)}(\sigma)$	$a_1(\sigma)$	$a_2(\sigma)$	$a_3(\sigma)$	$a_4(\sigma)$	$a_5(\sigma)$
0.1	L_{I}	61	.434(0)	.440(0)	.450(0)	−.162(−1)	.437(−2)	−.313(−3)	−.159(−3)	.565(−5)
		69	.375(0)	.316(0)	.321(0)	.121(0)	.211(−1)	−.171(−2)	−.581(−2)	.351(−4)
		81	.986(0)	.101(1)	.103(1)	.390(0)	.391(−1)	−.376(−2)	−.189(−1)	.907(−4)
		88	.330(1)	.272(1)	.277(1)	.408(0)	.420(−1)	−.438(−2)	−.212(−1)	.115(−3)
		95	.717(1)	.650(1)	.667(1)	.430(0)	.478(−1)	−.540(−2)	−.241(−1)	.153(−3)
	L_{II}	61	.985(1)	.855(1)	.844(1)	.267(−1)	.192(−3)	−.165(−4)	−.115(−2)	.358(−6)
		69	.173(2)	.178(2)	.177(2)	.405(−1)	.432(−3)	−.420(−4)	−.197(−2)	.101(−5)
		81	.916(2)	.951(2)	.508(2)	.732(−1)	.137(−2)	−.154(−3)	−.412(−2)	.436(−5)
		88	.499(2)	.529(2)	.943(2)	.104(0)	.278(−2)	−.339(−3)	−.638(−2)	.103(−4)
		95	.170(3)	.173(3)	.175(3)	.144(0)	.529(−2)	−.692(−3)	−.947(−2)	.226(−4)
	L_{III}	61	.103(2)	.107(2)	.104(2)	−.150(−1)	.119(−3)	.101(−4)	−.690(−3)	.216(−6)
		69	.200(2)	.200(2)	.200(2)	−.238(−1)	.283(−3)	.270(−4)	−.121(−2)	.648(−6)
		81	.507(2)	.512(2)	.500(2)	−.466(−1)	.990(−3)	.109(−3)	−.272(−2)	.305(−5)
		88	.859(2)	.842(2)	.836(2)	−.703(−1)	.212(−2)	.255(−3)	−.441(−2)	.768(−5)
		95	.146(3)	.139(3)	.139(3)	−.103(0)	.433(−2)	−.558(−3)	−.691(−2)	.180(−4)
1.0	L_{I}	61	.109(−2)	.118(−2)	.111(−2)	.229(−1)	.307(−2)	−.244(−3)	−.142(−2)	.492(−5)
		69	.162(−2)	.167(−2)	.160(−2)	.503(−1)	.674(−2)	−.605(−3)	−.303(−2)	.137(−4)
		81	.288(−2)	.284(−2)	.278(−2)	.140(0)	.205(−1)	−.215(−2)	−.864(−2)	.569(−4)
		88	.447(−2)	.404(−2)	.402(−2)	.241(0)	.389(−1)	−.443(−2)	−.153(−1)	.127(−3)
		95	.771(−2)	.607(−2)	.620(−2)	.376(0)	.668(−1)	−.819(−2)	−.248(−1)	.252(−3)
	L_{II}	61	.286(−3)	.299(−3)	.283(−3)	.651(−1)	.135(−2)	−.127(−3)	−.312(−2)	.302(−5)
		69	.661(−3)	.680(−3)	.654(−3)	.902(−1)	.251(−2)	−.264(−3)	−.483(−2)	.699(−5)
		81	.224(−2)	.233(−2)	.216(−2)	.144(0)	.606(−2)	−.737(−3)	−.885(−2)	.224(−4)
		88	.456(−2)	.475(−2)	.432(−2)	.192(0)	.105(−1)	−.138(−2)	−.127(−1)	.454(−4)
		95	.982(−2)	.952(−2)	.873(−2)	.249(0)	.172(−1)	−.241(−2)	−.176(−1)	.849(−4)
	L_{III}	61	.171(−3)	.181(−3)	.171(−3)	−.244(−1)	.704(−3)	.553−(4)	−.114(−2)	.111(−5)
		69	.333(−3)	.348(−3)	.329(−3)	−.368(−1)	.142(−2)	.126(−3)	−.191(−2)	.286(−5)
		81	.825(−3)	.832(−3)	.806(−3)	−.677(−1)	.399(−2)	.415(−3)	−.397(−2)	.109(−4)
		88	.136(−2)	.134(−2)	.131(−2)	−.984(−1)	.754(−2)	.850(−3)	−.617(−2)	.242(−4)
		95	.221(−2)	.218(−2)	.213(−2)	−.141(0)	.136(−1)	.165(−2)	−.935(−2)	.507(−4)

Table 6

The results of our recalculation for electric quadrupole ($E2$) transitions. The static particle parameters $b_2^{(0)}$ are presented together with the dynamic coefficients for the energies $k = 0.1$ and $k = 1.0$ ($m_e c^2$). In column 1 the results of SLIV and BAND (for the L_{I}- and L_{II}-subshells) and those of MIRANDA et al. (for the L_{III}-subshell) are given.

k ($m_e c^2$)	σ	Z	BAND et al. [29] MIRANDA et al. [30] $b_2(E2)$	$b_2^{(0)}(E2,\sigma)$	$c_1(\sigma)$	$c_2(\sigma)$	$c_3(\sigma)$	$c_4(\sigma)$	$c_5(\sigma)$
0.1	L_{I}	61	.171(1)	.171(1)	−.507(−1)	.357(−2)	−.247(−3)	.140(−2)	.433(−5)
		69	.118(1)	.119(1)	.343(−1)	.248(−1)	−.195(−2)	−.241(−2)	.389(−4)
		81	.125(1)	.125(1)	.412(0)	.438(−1)	−.410(−2)	−.195(−1)	.965(−4)
		88	.147(1)	.147(1)	.399(0)	.400(−1)	−.408(−2)	−.202(−1)	.104(−3)
		95	.157(1)	.157(1)	.406(0)	.425(−1)	−.471(−2)	−.223(−1)	.131(−3)
	L_{II}	61	.125(1)	.125(1)	.279(−1)	.213(−3)	−.184(−4)	−.120(−2)	.398(−6)
		69	.130(1)	.130(1)	.418(−1)	.465(−3)	−.451(−4)	−.203(−2)	.109(−5)
		81	.136(1)	.136(1)	.739(−1)	.141(−2)	−.158(−3)	−.416(−2)	.447(−5)
		88	.138(1)	.138(1)	.104(0)	.280(−2)	−.342(−3)	−.640(−2)	.104(−4)
		95	.140(1)	.140(1)	.144(0)	.525(−2)	−.688(−3)	−.944(−2)	.225(−4)
	L_{III}	61	.125(1)	.125(1)	−.154(−1)	0.000(0)	.969(−6)	−.710(−3)	.411(−7)
		69	.128(1)	.127(1)	−.231(−1)	0.000(0)	.218(−5)	−.119(−2)	.104(−6)
		81	.130(1)	.129(1)	−.414(−1)	.252(−8)	.674(−5)	−.245(−2)	.373(−6)
		88	.129(1)	.127(1)	−.590(−1)	.627(−8)	.137(−4)	−.377(−2)	.825(−6)
		95	.124(1)	.122(1)	−.815(−1)	.132(−7)	.252(−4)	−.556(−2)	.163(−5)
1.0	L_{I}	61		.139(1)	−.149(−1)	.309(−2)	−.236(−3)	.190(−4)	.456(−5)
		69		.131(1)	−.320(−2)	.731(−2)	−.631(−3)	−.712(−3)	.138(−4)
		81		.116(1)	.673(−1)	.254(−1)	−.257(−2)	−.500(−2)	.660(−4)
		88		.108(1)	.177(0)	.519(−1)	−.557(−2)	−.120(−1)	.159(−3)
		95		.104(1)	.354(0)	.901(−1)	−.107(−1)	−.236(−1)	.332(−3)
	L_{II}	61		.108(1)	.711(−1)	.180(−2)	−.168(−3)	−.339(−2)	.392(−5)
		69		.110(1)	.988(−1)	.327(−2)	−.341(−3)	−.525(−2)	.872(−5)
		81		.114(1)	.157(0)	.744(−2)	−.921(−3)	−.962(−2)	.270(−4)
		88		.117(1)	.209(1)	.126(−1)	−.168(−2)	−.138(−1)	.534(−4)
		95		.120(1)	.270(0)	.266(−1)	−.288(−2)	−.190(−1)	.976(−3)
	L_{III}	61		.871(0)	−.528(−1)	.126(−7)	.130(−4)	−.215(−2)	.490(−6)
		69		.891(0)	−.728(−1)	.282(−7)	.243(−4)	−.337(−2)	.108(−5)
		81		.910(0)	−.114(0)	.105(−6)	.608(−4)	−.619(−2)	.316(−5)
		88		.898(0)	−.148(0)	.255(−6)	.109(−3)	−.897(−2)	.615(−5)
		95		.887(0)	−.188(0)	.509(−6)	.176(−3)	−.120(−1)	.107(−4)

Table 7

The results of our recalculation for magnetic dipole ($M1$) transitions. The present conversion coefficients are presented in columns 3–5 for the energies $k = 0.1$ and $k = 1.0$ ($m_e c^2$). For comparison the results of ROSE and SLIV are given in columns 1 and 2, respectively. The present particle parameters are given in columns 7–9. The results of SLIV and BAND (L_I and L_{II}), and of MIRANDA et al. (L_{III}) are shown in column 6.

k ($m_e c^2$)	σ	Z	ROSE [13] β_1	SLIV [14] β_1	$\beta_1^{(0)}(\sigma)$	$b_1(\sigma)$	$b_2(\sigma)$	BAND et al. MIRANDA et al. [29, 30] $b_2(M1)$	$b_2^{(0)}(M1, \sigma)$	$c_1(\sigma)$	$c_2(\sigma)$
0.1	L_I	61	.106(1)	.121(1)	.120(1)	−.201(−1)	.101(−3)	−.200(−2)	−.155(−2)	−.557(−2)	.171(−5)
		69	.238(1)	.262(1)	.259(1)	−.290(−1)	.210(−3)	−.100(−1)	−.796(−2)	−.149(−1)	.111(−4)
		81	.746(1)	.801(1)	.816(1)	−.482(−1)	.582(−3)	−.470(−2)	−.450(−2)	−.292(−1)	.125(−3)
		88	.162(2)	.156(2)	.161(2)	−.653(−1)	.106(−2)	.130(−2)	.115(−2)	.196(−2)	−.113(−2)
		95	.372(2)	.316(2)	.327(2)	−.856(−1)	.183(−2)	.740(−2)	.733(−2)	−.343(−1)	−.366(−3)
	L_{II}	61	.823(−1)	.105(0)	.100(0)	−.420(−2)	.448(−5)	.346(0)	.351(0)	−.243(−2)	.461(−6)
		69	.189(0)	.236(0)	.236(0)	−.728(−2)	.134(−4)	.318(0)	.313(0)	−.419(−2)	.132(−5)
		81	.728(0)	.844(0)	.835(0)	−.157(−1)	.629(−4)	.259(0)	.255(0)	−.896(−2)	.580(−5)
		88	.135(1)	.178(1)	.180(1)	−.248(−1)	.155(−3)	.219(0)	.217(0)	−.140(−1)	.144(−4)
		95	.344(1)	.390(1)	.405(1)	−.375(−1)	.354(−3)	.179(0)	.176(0)	−.210(−1)	.326(−4)
	L_{III}	61	.183(−1)	.201(−1)	.193(−1)			.727(0)	.930(0)		
		69	.324(−1)	.357(−1)	.347(−1)			.655(0)	.947(0)		
		81	.731(−1)	.773(−1)	.753(−1)			.569(0)	.951(0)		
		88	.113(0)	.115(0)	.113(0)			.517(0)	.947(0)		
		95	.153(0)	.168(0)	.166(0)			.939(0)	.938(0)		
1.0	L_I	61	.203(−2)	.209(−2)	.203(−2)	−.231(−1)	.139(−3)		.396(0)	−.136(−1)	.560(−5)
		69	.394(−2)	.422(−2)	.415(−2)	−.338(−1)	.294(−3)		.294(0)	−.194(−1)	.131(−4)
		81	.117(−1)	.123(−1)	.122(−1)	−.566(−1)	.811(−3)		.161(0)	−.318(−1)	.419(−4)
		88	.255(−1)	.232(−1)	.234(−1)	−.763(−1)	.146(−2)		.103(0)	−.429(−1)	.906(−4)
		95	.582(−1)	.451(−1)	.465(−1)	−.992(−1)	.247(−2)		.549(−1)	−.562(−1)	.174(−3)
	L_{II}	61	.108(−3)	.134(−3)	.113(−3)	−.124(−1)	.395(−4)		.376(0)	−.753(−2)	.565(−5)
		69	.262(−3)	.326(−3)	.292(−3)	−.191(−1)	.927(−4)		.333(0)	−.114(−1)	.131(−4)
		81	.112(−2)	.123(−2)	.117(−2)	−.346(−1)	.303(−3)		.262(0)	−.205(−1)	.429(−4)
		88	.241(−2)	.271(−2)	.266(−2)	−.491(−1)	.609(−3)		.214(0)	−.291(−1)	.906(−4)
		95	.684(−2)	.620(−2)	.632(−2)	−.673(−1)	.114(−2)		.171(0)	−.397(−1)	.174(−3)
	L_{III}	61	.218(−4)	.245(−4)	.217(−4)				.932(0)		
		69	.390(−4)	.420(−4)	.390(−4)				.902(0)		
		81	.833(−4)	.871(−4)	.838(−4)				.916(0)		
		88	.121(−3)	.131(−3)	.124(−3)				.925(0)		
		95	.172(−3)	.192(−3)	.180(−3)				.931(0)		

Table 8

The results of our recalculation for magnetic quadrupole ($M2$) transitions. The present conversion coefficients are presented in columns 3–5 for the energies $k = 0.1$ and $k = 1.0$ ($m_e c^2$). For comparison the results of ROSE and SLIV are given in columns 1 and 2, respectively. The present particle parameters are given in columns 7–9. The results of SLIV and BAND (L_I and L_{II}), and of MIRANDA et al. (L_{III}) are shown in column 6.

k ($m_e c^2$)	σ	Z	ROSE [13] β_2	SLIV [14] β_2	$b_2^{(0)}(\sigma)$	$b_1(\sigma)$	$b_2(\sigma)$	BAND et al. MIRANDA et al. [29, 30] $b_2(M2)$	$b_2^{(0)}(M2, \sigma)$	$c_1(\sigma)$	$c_2(\sigma)$
0.1	L_I	61	.335(2)	.338(2)	.338(2)	−.162(−1)	.656(−4)	.139(1)	.139(1)	−.162(−1)	.657(−4)
		69	.786(2)	.772(2)	.770(2)	−.227(−1)	.128(−3)	.140(1)	.140(1)	−.226(−1)	.128(−3)
		81	.269(3)	.253(3)	.252(3)	−.361(−1)	.326(−3)	.140(1)	.140(1)	−.361(−1)	.326(−3)
		88	.569(3)	.485(3)	.499(3)	−.478(−1)	.573(−3)	.140(1)	.140(1)	−.478(−1)	.572(−3)
		95	.123(4)	.960(3)	.990(3)	−.614(−1)	.942(−3)		.139(1)	−.614(−1)	.943(−3)
	L_{II}	61	.334(1)	.344(1)	.338(1)	−.226(−2)	.129(−5)	.129(1)	.129(1)	−.234(−2)	.138(−5)
		69	.707(1)	.725(1)	.720(1)	−.379(−2)	.362(−5)	.130(1)	.130(1)	−.391(−2)	.387(−5)
		81	.224(1)	.206(2)	.208(2)	−.782(−2)	.154(−4)	.131(1)	.131(1)	−.805(−2)	.163(−4)
		88	.480(2)	.371(2)	.382(2)	−.120(−1)	.364(−4)	.131(1)	.132(1)	−.123(−1)	.384(−4)
		95	.723(2)	.675(2)	.695(2)	−.178(−1)	.801(−4)		.132(1)	−.182(−1)	.840(−4)
	L_{III}	61	.110(2)	.112(2)	.107(2)	−.162(−1)	.680(−4)	.880(−2)	.174(−1)	−.290(−2)	0
		69	.286(2)	.273(2)	.272(2)	−.229(−1)	.134(−3)	.398(−1)	.649(−1)	−.102(−1)	0
		81	.111(3)	.985(2)	.100(3)	−.368(−1)	.343(−3)	.667(−1)	.106(0)	−.177(−1)	.356(−8)
		88	.242(3)	.202(3)	.207(3)	−.489(−1)	.604(−3)	.746(−1)	.116(0)	−.238(−1)	.788(−8)
		95	.524(3)	.397(3)	.423(3)	−.629(−1)	.995(−3)	.741(−1)	.116(0)	−.308(−1)	.148(−7)
1.0	L_I	61	.696(−2)	.701(−2)	.689(−2)	−.173(−1)	.781(−4)		.123(1)	−.184(−1)	.885(−4)
		69	.145(−1)	.140(−1)	.139(−1)	−.246(−1)	.155(−3)		.126(1)	−.258(−1)	.171(−3)
		81	.426(−1)	.391(−1)	.397(−1)	−.395(−1)	.395(−3)		.131(1)	−.408(−1)	.420(−3)
		88	.849(−1)	.715(−1)	.733(−1)	−.523(−1)	.690(−3)		.133(1)	−.536(−1)	.722(−3)
		95	.171(0)	.132(0)	.137(0)	−.669(−1)	.112(−2)		.135(1)	−.680(−1)	.116(−2)
	L_{II}	61	.620(−3)	.662(−3)	.618(−3)	−.697(−2)	.123(−4)		.128(1)	−.724(−2)	.133(−4)
		69	.149(−2)	.159(−2)	.151(−2)	−.104(−1)	.274(−4)		.128(1)	−.108(−1)	.294(−4)
		81	.560(−2)	.547(−2)	.542(−2)	−.182(−1)	.839(−4)		.130(1)	−.188(−1)	.892(−4)
		88	.118(−1)	.112(−1)	.113(−1)	−.255(−1)	.164(−3)		.131(1)	−.262(−1)	.173(−3)
		95	.261(−1)	.231(−1)	.238(−1)	−.346(−1)	.301(−3)		.132(1)	−.354(−1)	.316(−3)
	L_{III}	61	.197(−3)	.196(−3)	.190(−3)	−.155(−1)	.905(−4)		+.173(−1)	−.285(−2)	.167(−9)
		69	.462(−3)	.444(−3)	.435(−3)	−.235(−1)	.189(−3)		−.259(0)	−.241(−1)	.582(−8)
		81	.161(−2)	.141(−2)	.141(−2)	−.408(−1)	.510(−3)		−.138(0)	−.410(−1)	.305(−7)
		88	.335(−2)	.274(−2)	.276(−2)	−.558(−1)	.910(−3)		−.605(−1)	−.694(−1)	.852(−7)
		95	.683(−2)	.528(−2)	.538(−2)	−.732(−1)	.150(−2)		+.143(−1)	−.191(−6)	−.191(−6)

The surface model (SM) leads to the nuclear parameters $\lambda_i = 1$ (see section IV) and is included in $\beta_L(\sigma)_{SM}$.

A similar result has been obtained by HAGER and SELTZER [27], who used a screening function, obtained by non-relativistic Hartree-Fock calculations [28].

The recalculated particle parameters of the K, L_{I} and L_{II} shell agree very well with the values of SLIV and BAND [29], as can be seen in Tables 3–8, where we show our results in the notation of Eq. (50)–(53). An investigation of the dynamic coefficients and of the anomaly factor $\bar{\Delta}$, as defined in Eq. (52a) shows, that the particle parameters may also depend considerably on nuclear structure effects. The fact, that

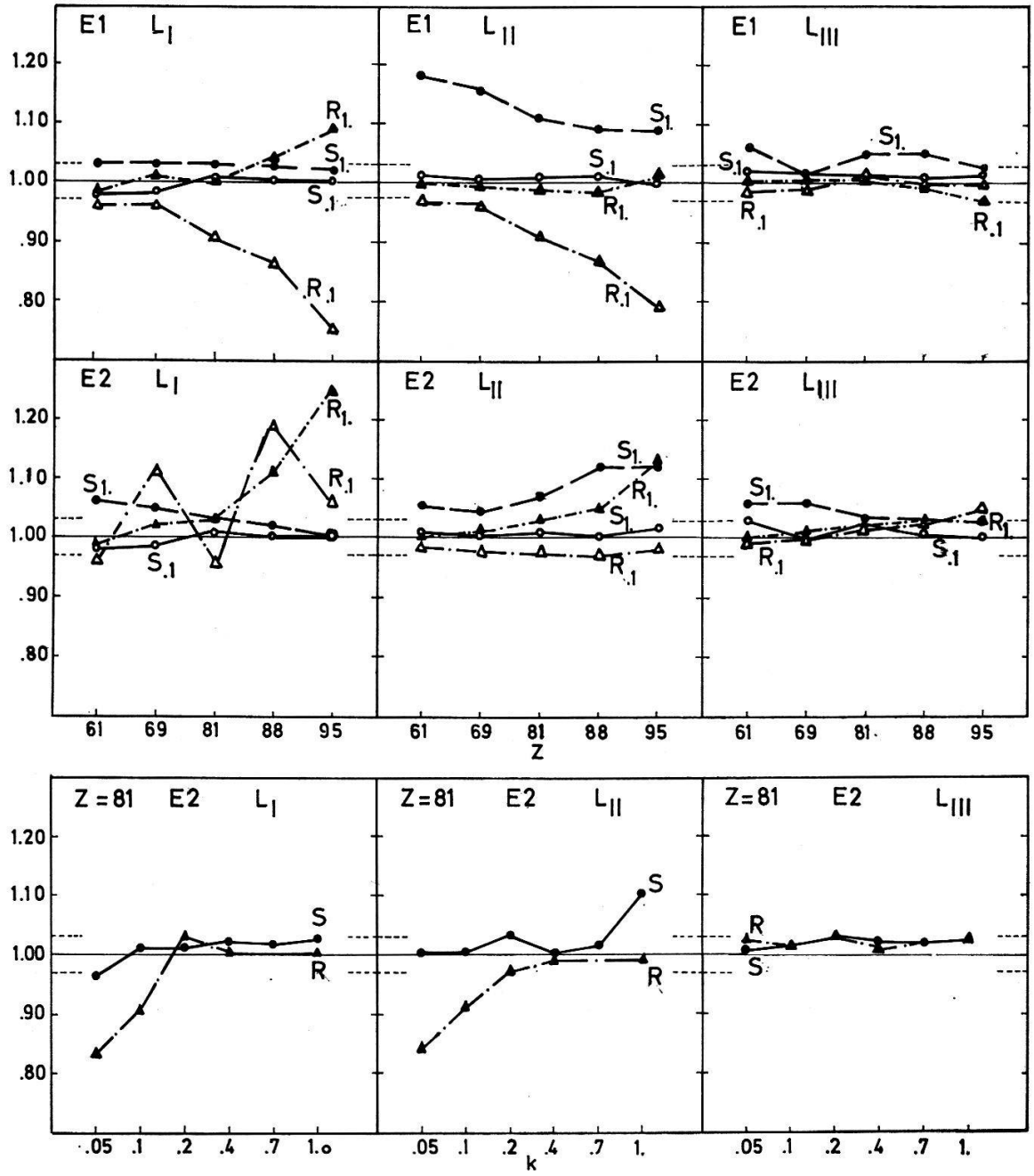

Figure 1

Comparison of the present conversion coefficients with those of ROSE (R) and those of SLIV (S) for electric dipole and electric quadrupole transitions. The indices .1 and 1. represent the energies $k = 0.1$ and $k = 1.0$ $(m_e c^2)$, respectively.

most particle parameters are normal within the limits of error is regarded to be accidental. For the L_{III} shell we have compared our results with the recent calculation by MIRANDA et al. [30]. We agree well with the particle parameters of electric transitions. There is, however, not as well for magnetic transitions.

We have performed a recalculation of the K- and L-shell matrix elements and phases for electric as well as magnetic transitions. We have restricted ourselves to medium and heavy nuclear charge numbers and to small energies, where possible large penetration effects may be significant. We have chosen the following values of nuclear charges:

$$Z = 60, 64, \ldots 96$$

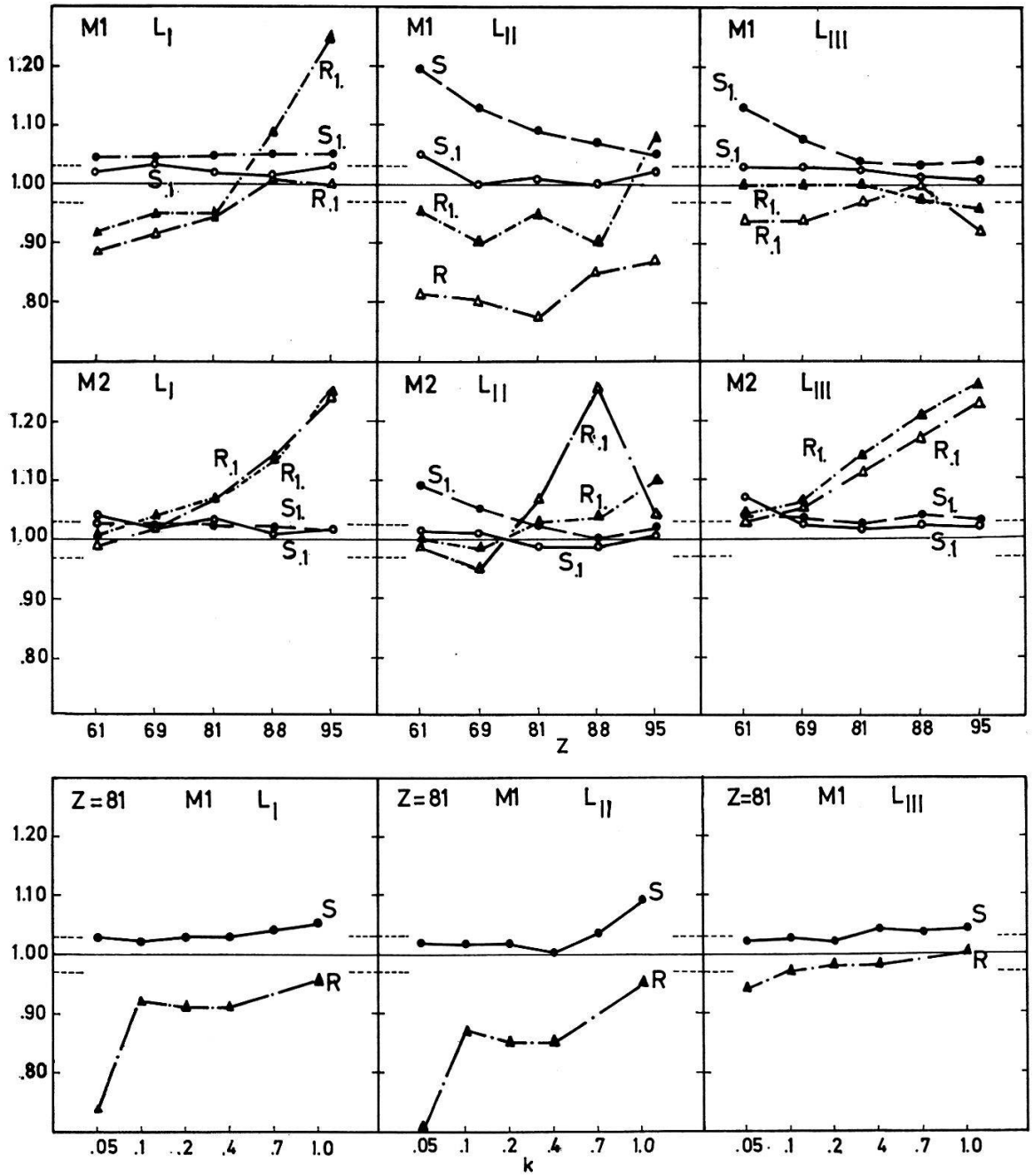

Figure 2

Comparison of the present conversion coefficients with those of ROSE (R) and those of SLIV (S) for magnetic dipole and magnetic quadrupole transitions. The indices .1 and 1. represent the energies $k = 0.1$ and $k = 1.0$ $(m_e c^2)$, respectively.

and the following energies:

$$k = .02,\ .05,\ .10,\ .15,\ .20,\ .30,\ .40,\ .50,\ .70,\ 1.0\ .$$

Furthermore we have calculated the M-shell conversion coefficients and particle parameters including screening (TFD) and all finite nuclear size effects from

$$Z = 72,\ 76,\ \ldots,\ 96$$

The results of this calculation will be published separately.

About a dozen of highly hindered E1 transitions with anomalous conversion coefficients or particle parameters have been investigated using our recalculated values [31].

Acknowledgements

The author likes to thank Prof. ROLF M. STEFFEN to have suggested this work. He is indebted to Prof. KURT ALDER for his kind support and interest during the course of this work, as well as for many instructive discussions. The computations on a UNIVAC 1107 were enabled by a grant of the UNIVAC Switzerland, Inc., and the "Arithma Rechenzentrum" in Zürich-Switzerland, and are acknowledged thankfully.

VI. Appendixes

Appendix 1

Although the solutions of the Dirac equation for a central field are described often in the literature [20], we shall give here a short survey and define the notation.

The Dirac equation

$$(\boldsymbol{\alpha}\,\boldsymbol{p} + \beta + V(r))\,\psi = W\,\psi\,, \tag{A1}$$

with the momentum operator p and the total energy $W = \sqrt{p^2 + 1}$, has for the central field $V(r)$ the particular spinor solution designed by

$$|\,\varkappa\,\mu\rangle = \frac{1}{r}\begin{pmatrix} \Phi^{\mu}_{\varkappa}\ u_{\varkappa}(r) \\ -\,S(\varkappa)\ \Phi^{\mu}_{-\varkappa}\ v_{\varkappa}(r) \end{pmatrix}. \tag{A2}$$

The 4-component spinor as well as the two component spinor $\Phi^{\mu}_{\varkappa}$ obey the "Convention T" (cf. ref. [10]). This two component spinor is defined by

$$\Phi^{\mu}_{\varkappa} = \sum_{\tau} \langle l\,\mu - \tau\,{}^1\!/_2\,\tau\,|\,j\,\mu\rangle\, i^l\, Y_{l,\,\mu-\tau}(\hat{r})\ \chi^{\tau} \tag{A3}$$

with

$$\chi^{1/2} = \begin{pmatrix} 1 \\ 0 \end{pmatrix} \qquad \chi^{-1/2} = \begin{pmatrix} 0 \\ 1 \end{pmatrix}.$$

The Dirac quantum number $\varkappa$ is the eigenvalue of the equation

$$-\,(\boldsymbol{\sigma}\,\boldsymbol{L} + 1)\ \Phi^{\mu}_{\varkappa} = \varkappa\,\Phi^{\mu}_{\varkappa} \tag{A4}$$

and replaces the orbital quantum number l in the unrelativistic theory. It is restricted to all positive and negative integers except zero, i.e.

$$\varkappa = l\,(l+1) - (j + {}^1\!/_2)^2$$

or

$$l = \varkappa \quad \text{for} \quad \varkappa > 0 \qquad l = -\varkappa - 1 \quad \text{for} \quad \varkappa < 0\,. \tag{A5}$$

Sometimes the quantity $\bar{l} = l - S(\varkappa)$ is used.

The sign of $\varkappa$ is designed by $S(\varkappa)$.

The spinor $\Phi^{\mu}_{\varkappa}$ has further the property

$$i\,\boldsymbol{\sigma}\,\hat{\boldsymbol{r}}\,\Phi^{\mu}_{\varkappa} = S(\varkappa)\,\Phi^{\mu}_{-\varkappa}\,. \tag{A6}$$

The matrix elements containing these spinors can be easily evaluated. We get for the angular matrix element of the electric transitions

$$\langle \Phi^{\mu}_{\varkappa} \mid i^{L}\,Y_{LM} \mid \Phi^{\mu_i}_{\varkappa_i} \rangle = (-)^{\mu-1/2}\,i^{l_i+L-l}\sqrt{\frac{2L+1}{4\pi}}$$
$$\times\sqrt{(2j_i+1)\,(2j+1)\,(2l_i+1)\,(2l+1)}\begin{pmatrix} l_i & l & L \\ 0 & 0 & 0 \end{pmatrix}\begin{pmatrix} j_i & L & j \\ \mu_i & M & -\mu \end{pmatrix}\begin{Bmatrix} l_i & l & L \\ j & j_i & 1/2 \end{Bmatrix}. \tag{A7}$$

For magnetic transitions $\varkappa$ has to be replaced by $-\varkappa$ in Eq. (A 6). Thus we can replace in Eq. (A 7) l by $\bar{l}$ to get the right selection rules for magnetic transitions. The use of (A 23) leads finally to

$$\langle \Phi^{\mu}_{\varkappa} \mid i^{L}\,Y_{LM} \mid \Phi^{\mu_i}_{\varkappa_i} \rangle = (-)^{\mu+1/2}\,i^{l_i+L-l}\sqrt{\frac{(2L+1)}{4\pi}}\sqrt{(2j+1)\,(2j_i+1)}$$
$$\times\begin{pmatrix} j_i & j & L \\ 1/2 & -1/2 & 0 \end{pmatrix}\begin{pmatrix} j_i & L & j \\ \mu_i & M & -\mu \end{pmatrix} \tag{A8}$$

for the electric transitions.

In Eq. (A 2) the radial functions $u_{\varkappa}$ and $v_{\varkappa}$ are real and solutions of the equations

$$\frac{du_{\varkappa}}{dr} = -\frac{\varkappa}{r}\,u_{\varkappa} + (W + 1 - V(r))\,v_{\varkappa} \qquad \frac{dv_{\varkappa}}{dr} = \frac{\varkappa}{r}\,v_{\varkappa} - (W - 1 - V(r))\,u_{\varkappa}. \tag{A9}$$

The asymptotic behaviour of the radial functions is given by

$$u_{\varkappa} \longrightarrow \sqrt{\frac{W+1}{\pi p}}\,\cos\left(p\,r + \Delta_{\varkappa} + \delta_{\varkappa}(0)\right)$$
$$v_{\varkappa} \longrightarrow -\sqrt{\frac{W-1}{\pi p}}\,\sin\left(p\,r + \Delta_{\varkappa} + \delta_{\varkappa}(0)\right); \qquad \delta_{\varkappa}(0) = -\frac{l+1}{2}\,\pi \tag{A10}$$

where phase $\Delta_{\varkappa}$ depends on the specific potential and is zero in a $Z = 0$ approximation i.e.

$$\Delta_{\varkappa}\,(Z = 0) = 0$$

For large distances the electron behaves like a plane wave carrying the intrinsic spin orientation τ. This plane wave can be expanded into the particular "spherical waves" $|\,\varkappa\,\mu\rangle$ of Eq. (A 2), i.e.

$$|\,\boldsymbol{p}, \tau\rangle = N \sum_{\varkappa\mu} s_{\varkappa}\,a_{\varkappa\mu}(\tau)\;|\,\varkappa\,\mu\rangle \tag{A11}$$

with

$$s_{\varkappa} = e^{-i\Delta_{\varkappa}} \qquad a_{\varkappa\mu} = \sqrt{\frac{2l+1}{4\pi}}\,\langle l\,\mu - \tau\,1/2\,\tau \mid j\,\mu\rangle\,D^{l}_{0\,\mu-\tau}\,(\hat{p} \longrightarrow \hat{z})\,. \tag{A12}$$

The overall factor N is fixed by the asymptotic behaviour (A 10).

Appendix 2

In chapter IV we have taken into account the finite nuclear size by the assumption of a sharp edged sphere of radius R with homogeneous charge distribution. Inside this nucleus the potential $V(r)$ of the electron is described by

$$V(r) = -\frac{Z\alpha}{2R}(3 - x^2); \qquad x = \frac{r}{R}. \tag{A13}$$

The solutions of the Dirac equation (A 9) in this potential are wel-lknown, and can be given as a power series [20]. For $\varkappa > 0$, $k = |\varkappa|$ we have

$$u_\varkappa = x^{k+1} \sum_{n=0}^{\infty} a_n x^{2n}; \qquad v_\varkappa = x^k \sum_{n=0}^{\infty} b_n x^{2n}. \tag{A14}$$

The coefficients a_n and b_n are related through the recursion relations

$$\begin{aligned}(2k + 2n + 1)\, a_n &= \left[R(W + 1) + \frac{3\alpha Z}{2}\right] b_n - \frac{\alpha Z}{2} b_{n-1} \\ 2(n + 1)\, b_{n+1} &= -\left[R(W - 1) + \frac{3\alpha Z}{2}\right] a_n + \frac{\alpha Z}{2} a_{n-1}\end{aligned} \tag{A15}$$

with

$$a_0 = \frac{R(W+1) + (3\alpha Z/2)}{2k+1} b_0 .$$

For $\varkappa < 0$ we obtain the solutions by interchanging u_x and v_x in (A 14) and by replacing in (A 15) the charge Z and the energy W by their negative values.

In the following we compile the different radial functions $g^{(i)}_{\varkappa\varkappa_i}(r)$ $(i = 1,3)$ and their explicit dependence on the coefficients a_n and b_n. Let us consider the following expression:

$$u_{\varkappa_i} v_\varkappa - v_{\varkappa_i} u_\varkappa = x^p \sum_{m=0}^{\infty} \alpha_m x^{2m}$$

with

$$\alpha_m = \begin{cases} S_{(\varkappa_i)} \sum_{n=0}^{m} a_n B_{m-n} - b_n A_{m-n}; & \varkappa\varkappa_i > 0 \\ S_{(\varkappa_i)} \sum_{n=0}^{m} a_{n-1} A_{m-n} - b_n B_{m-n}; & \varkappa\varkappa_i < 0 . \end{cases} \tag{A16}$$

Here and in the following the solution of the recursion relations (A 15), for the bound states and for the continuum states are denoted by minor and capital letters, respectively. The quantities p and $\bar{p}$ are defined in Eq. (41). For the similar expressions occurring in the definition of the functions $g(r)$ we get

$$u_{\varkappa_i} v_\varkappa + v_{\varkappa_i} u_\varkappa = x^p \sum_{m=0}^{\infty} \beta_m x^{2m}$$

with

$$\beta_m = \begin{cases} \sum_{n=0}^{m} a_n B_{m-n} + b_n A_{m-n}; & \varkappa\varkappa_i > 0 \\ \sum_{n=0}^{m} a_{n-1} A_{m-n} + b_n B_{m-n}; & \varkappa\varkappa_i < 0 \end{cases} \tag{A17}$$

and

$$u_{\varkappa_i} u_\varkappa + v_{\varkappa_i} v_\varkappa = x^{\bar{p}} \sum_{m=0}^{\infty} \gamma_m x^{2m}$$

with

$$\gamma_m = \begin{cases} \sum_{n=0}^{m} a_{n-1} A_{m-n} + b_n B_{m-n}; & \varkappa \varkappa_i > 0 \\ \sum_{n=0}^{m} a_n B_{m-n} + b_n A_{m-n}; & \varkappa \varkappa_i < 0. \end{cases} \tag{A18}$$

Using these expressions we can write the radial functions as follows

$$g^{(1)}_{\varkappa \varkappa_i}(r) = \frac{i}{k} x^p \sum_{m=0}^{\infty} d_m x^{2m}$$

with

$$d_m = \begin{cases} -\alpha_m - kR \dfrac{(p+2m-1)\gamma_m - kR\alpha_{m-1}}{(p+2m)(p+2m-1) - L(L+1)} & \varkappa \varkappa_i > 0 \\ -\alpha_m - kR \dfrac{(p+2m-1)\gamma_{m-1} - kR\alpha_{m-1}}{(p+2m)(p+2m-1) - L(L+1)} & \varkappa \varkappa_i < 0 \end{cases} \tag{A19}$$

and

$$g^{(2)}_{\varkappa \varkappa_i}(r) = \frac{i}{k} x^{\bar{p}} \sum_{m=0}^{\infty} e_m x^{2m}$$

with

$$e_m = \begin{cases} \dfrac{-L(L+1)\gamma_m + kR(\bar{p}+2m+1)\alpha_{m-1}}{(\bar{p}+2m)(\bar{p}+2m+1) - L(L+1)}; & \varkappa \varkappa_i > 0 \\ \dfrac{-L(L+1)\gamma_m + kR(\bar{p}+2m+1)\alpha_m}{(\bar{p}+2m)(\bar{p}+2m+1) - L(L+1)}; & \varkappa \varkappa_i < 0 \end{cases} \tag{A20}$$

and finally

$$g^{(3)}_{\varkappa \varkappa_i}(r) = \frac{i}{k} x^p \sum_{m=0}^{\infty} f_m x^{2m}$$

with

$$f_m = \frac{\beta_m}{(p+2m)(p+2m+1) - L(L+1)}. \tag{A21}$$

Appendix 3

In the following, all expressions are based on the well-known relation [19]

$$\sum_{\mu_1 \mu_2 \mu_3} (-)^{l_1+l_2+l_3+\mu_1+\mu_2+\mu_3} \begin{pmatrix} j_1 & l_2 & l_3 \\ m_1 & \mu_2 & -\mu_3 \end{pmatrix} \begin{pmatrix} l_1 & j_2 & l_3 \\ -\mu_1 & m_2 & \mu_3 \end{pmatrix} \begin{pmatrix} l_1 & l_2 & j_3 \\ \mu_1 & -\mu_2 & m_3 \end{pmatrix} = \begin{pmatrix} j_1 & j_2 & j_3 \\ m_1 & m_2 & m_3 \end{pmatrix} \begin{Bmatrix} j_1 j_2 j_3 \\ l_1 l_2 l_3 \end{Bmatrix} \tag{A22}$$

and on the tables of selected $3j$- and $6j$-symbols (see e.g. EDMONDS).

With the special value $l_3 = {}^1/_2$ the useful relation

$$-\sqrt{(2l+1)(2l'+1)} \begin{pmatrix} l & l' & k \\ 0 & 0 & 0 \end{pmatrix} \begin{Bmatrix} l & l' & k \\ j' & j & {}^1/_2 \end{Bmatrix} = \begin{pmatrix} j & j' & k \\ {}^1/_2 & -{}^1/_2 & 0 \end{pmatrix} \tag{A23}$$

can be easily derived.

Furthermore, the recursion relation

$$\begin{aligned} &[j_3(j_3+1) - j_1(j_1+1) - j_2(j_2+1) - 2m_1 m_2] \begin{pmatrix} j_1 & j_2 & j_3 \\ m_1 & m_2 & m_3 \end{pmatrix} \\ &= \sqrt{(j_1+m_1)(j_1-m_1+1)(j_2-m_2)(j_2+m_1+1)} \begin{pmatrix} j_1 & j_2 & j_3 \\ m_1-1 & m_2+1 & m_3 \end{pmatrix} \\ &+ \sqrt{(j_1-m_1)(j_1+m_1+1)(j_2+m_2)(j_2-m_2+1)} \begin{pmatrix} j_1 & j_2 & j_3 \\ m_1+1 & m_2-1 & m_3 \end{pmatrix} \end{aligned} \tag{A24}$$

leads to the special relations (k even)

$$\begin{pmatrix} L & L & k \\ 0 & 0 & 0 \end{pmatrix} = -\left[1 + \frac{k\,(k+1)}{2\,L\,(L+1) - k\,(k+1)}\right] \begin{pmatrix} L & L & k \\ 1 & -1 & 0 \end{pmatrix} \tag{A25}$$

$$\begin{pmatrix} L & L & k \\ 2 & -2 & 0 \end{pmatrix} = -\left[1 + \frac{k\,(k+1)}{2\,L\,(L+1) - k\,(k+1)} \frac{k\,(k+1) - 3\,L\,(L+1)}{(L-1)\,(L+2)}\right] \begin{pmatrix} L & L & k \\ 1 & -1 & 0 \end{pmatrix} \tag{A26}$$

$$\begin{pmatrix} L & L' & k \\ 2 & -2 & 0 \end{pmatrix} = \frac{k\,(k+1) + 2 - L\,(L+1) - L'\,(L'+1)}{\sqrt{(L-1)\,(L+2)\,(L'-1)\,(L'+2)}} \begin{pmatrix} L & L' & k \\ 1 & -1 & 0 \end{pmatrix}. \tag{A27}$$

In order to extract the dependence on the tensor coupling constant k explicitely we can now express the geometrical factor

$$g(j_i, L, L') = (-)^{j_i - 1/2} \frac{\begin{pmatrix} j & j' & k \\ 1/2 & -1/2 & 0 \end{pmatrix} \begin{Bmatrix} j & j' & k \\ L' & L & j_i \end{Bmatrix}}{\begin{pmatrix} L & L' & k \\ 1 & -1 & 0 \end{pmatrix}}.$$

In the case of $j_i = 1/2$ we obtain

$$g(1/2, L, L) = \frac{\delta_{jj'}}{2\,j+1} + \frac{k\,(k+1)}{2\,L\,(L+1) - k\,(k+1)} \frac{+1}{2\,L\,(L+1)} \tag{A28}$$

and

$$g(1/2, L, L') = (-)^{j+j'+1} \sqrt{\frac{(2\,L - j + 1/2)\,(2\,L' - j' + 1/2)}{(2\,j+1)\,(2\,L+1)\,(2\,j'+1)\,(2\,L'+1)}}. \tag{A29}$$

In a similar way we obtain for $j_i = 3/2$ and pure multipoles i.e. $L = L'$

$$\begin{aligned} g(3/2, L, L) = {} & \frac{\delta_{jj'}}{2\,j+1} + \frac{k\,(k+1)}{2\,L\,(L+1) - k\,(k+1)} \begin{pmatrix} L & j & 3/2 \\ 0 & -1/2 & 1/2 \end{pmatrix} \begin{pmatrix} L & j' & 3/2 \\ 0 & -1/2 & 1/2 \end{pmatrix} \\ & + \frac{k\,(k+1)}{2\,L\,(L+1) - k\,(k+1)} \frac{k\,(k+1) - 3\,L\,(L+1)}{(L-1)\,(L+2)} \begin{pmatrix} L & j' & 3/2 \\ 2 & -1/2 & -3/2 \end{pmatrix} \begin{pmatrix} L & j & 3/2 \\ 2 & -1/2 & -3/2 \end{pmatrix} \end{aligned} \tag{A30}$$

and for the mixed multipoles, i.e. $L + L'$ odd,

$$g(3/2, L, L') = C^{(1)}(j, j') + k\,(k+1)\,C^{(2)}(j\,j') \tag{A31}$$

with

$$\begin{aligned} C^{(1)}(j\,j') = {} & \begin{pmatrix} j & L & 3/2 \\ 1/2 & -1 & 1/2 \end{pmatrix} \begin{pmatrix} j' & L' & 3/2 \\ 1/2 & -1 & 1/2 \end{pmatrix} - \begin{pmatrix} L & j & 3/2 \\ -1 & -1/2 & 3/2 \end{pmatrix} \begin{pmatrix} L' & j' & 3/2 \\ -1 & -1/2 & 3/2 \end{pmatrix} \\ & + \frac{L\,(L+1) + L'\,(L'+1) - 2}{\sqrt{(L-1)\,(L+2)\,(L'-1)\,(L'+2)}} \begin{pmatrix} j & L & 3/2 \\ 1/2 & -2 & 3/2 \end{pmatrix} \begin{pmatrix} j' & L' & 3/2 \\ 1/2 & -2 & 3/2 \end{pmatrix} \end{aligned} \tag{A32}$$

and

$$C^{(2)}(j\,j') = \frac{-1}{\sqrt{(L-1)\,(L+2)\,(L'-1)\,(L'+2)}} \begin{pmatrix} j & L & 3/2 \\ 1/2 & -2 & 3/2 \end{pmatrix} \begin{pmatrix} j' & L' & 3/2 \\ 1/2 & -2 & 3/2 \end{pmatrix}$$

References

[1] M. E. Rose, G. H. Goertzel, B. I. Spinrad, J. Harr and P. Strong, Phys. Rev. *79*, 79 (1951).
[2] E. L. Church and J. Weneser, Phys. Rev. *104*, 1382 (1956).
[3] E. L. Church and J. Weneser, *Nuclear Structure Effects in Internal Conversion*, Ann. Rev. Nucl. Sci. *10*, 193 (1960).
[4] T. A. Green and M. E. Rose, Phys. Rev. *110*, 105 (1958).
[5] E. L. Church and J. Weneser, Nucl. Phys. *28*, 602 (1961).
[6] G. Kramers and S. G. Nilsson, Nucl. Phys. *35*, 273 (1962).
[7] F. Asaro, F. S. Stephens jr., J. M. Hollander and I. Perlman, Phys. Rev. *107*, 492 (1960).
[8] H. Frauenfelder, R. Steffen, *Angular Correlations, in Alpha-, Beta-, Gamma-Ray Spectroscopy*, Vol. 2, ed. K. Siegbahn (North Holland Publishing Co., Amsterdam Netherlands, 1965).
[9] L. C. Biedenharn and M. E. Rose, Rev. mod. Phys. *25*, 729 (1953).
[10] L. C. Biedenharn and M. E. Rose, Phys. Rev. *134*, B8 (1964).
[11] E. L. Church, A. Schwarzschild and J. Weneser, Phys. Rev. *133*, B35 (1964).
[12] E. V. Ivash, Nuovo Cim. IX, *136* (1958).
[13] M. E. Rose, *Internal Conversion Coefficients* (North Holland Publishing Co., Amsterdam, Netherlands, 1958).
[14] L. A. Sliv and I. M. Band, *Tables of Internal Conversion Coefficients in Alpha-, Beta-, Gamma-Ray Spectroscopy*, K. Siegbahn, ed. (North Holland Publishing Co., Amsterdam, Netherlands, 1965).
[15] See e.g. W. Franz, Z. Phys. *127*, 363 (1950); B. Stech, Z. Naturf. *7a*, 401 (1952).
[16] M. E. Rose, *Multipole Fields* (Wiley, New York, 1955).
[17] L. I. Schiff, *Quantum Mechanics* (McGraw-Hill Book Co., New York, 1965).
[18] G. N. Watson, *Theory of Bessel Functions*, 2nd ed. (Cambridge University Press, New York, 1944), pp. 405 and 429.
[19] A. R. Edmonds, *Angular Momentum in Quantum Mechanics* (Princeton University Press).
[20] M. E. Rose, *Relativistic Electron Theory* (Wiley, New York, 1961).
[21] G. T. Emery and M. E. Perlman, Phys. Rev. *151*, 984 (1966).
[22] S. Hagström, C. Nordling and K. Siegbahn, *Tables of Electron Binding Energies in Alpha-, Beta-, Gamma-Ray Spectroscopy*, ed. K. Siegbahn (North Holland Publishing Co., Amsterdam, Netherlands, 1965).
[23] P. Henrici, *Discrete Variable Methods in Ordinary Differential Equations* (Wiley, New York, 1962); or P. Henrici, *Elements of Numerical Analysis* (Wiley, New York, 1964).
[24] P. Gombas, *Die statistische Theorie des Atoms* (Springer, Wien, 1964).
[25] T. Novakov and J. M. Hollander, Nucl. Phys. *60*, 593 (1964).
[26] C. P. Bhalla, M. S. Freedman, F. T. Porter and F. Wagner (Preprint, Aug. 1966).
[27] E. Seltzer and R. Hager, Phys. Lett. *18*, 163 (1965).
[28] F. Herman and S. Skillman, *Atomic Structure Calculations* (Prentice Hall, 1963).
[29] I. M. Band, M. A. Listengarten, L. A. Sliv and J. E. Thun, in *Alpha-, Beta-, Gamma-Ray Spectroscopy*, ed. K. Siegbahn (North Holland Publishing Co., Amsterdam, Netherlands, 1965).
[30] A. Miranda, P. Hornshoj and B. I. Deutsch in *Internal conversion processes*, ed. J. Hamilton (Academic Press, New York, 1966).
[31] C. Pauli and K. Alder, Z. Physik *202*, 255 (1967).